2013

Synthesis and Electrodeposition of Mixed Metal Trinuclear Clusters of Molybdenum and Chromium in Ionic Liquid onto a Platinum Electrode

Lynn Renee Frock
Wright State University

SYNTHESIS AND ELECTRODEPOSITION OF MIXED METAL TRINUCLEAR CLUSTERS OF MOLYBDENUM AND CHROMIUM IN IONIC LIQUID ONTO A PLATINUM ELECTRODE.

A thesis submitted in partial fulfillment
of the requirements for the degree of
Master of Science

By

Lynn Renee Frock
A.S., Chemistry, Sinclair Community College, 1996
B.S., Psychology, Kennesaw State University, 2003

2012
Wright State University

WRIGHT STATE UNIVERSITY

GRADUATE SCHOOL

DECEMBER 14, 2012

I HEREBY RECOMMEND THAT THE THESIS PREPARED UNDER MY SUPERVISION BY Lynn Renee Frock ENTITLED Synthesis and Electrodeposition of Mixed Metal Trinuclear Clusters of Molybdenum and Chromium in Ionic Liquid onto a Platinum Electrode BE ACCEPTED IN PARTIAL FULFILLMENT OF THE REQUIREMENTS FOR THE DEGREE OF Master of Science.

_____

Vladimir Katovic, Ph.D.
Thesis Director

_____

David A. Grossie, Ph.D., Chair
Department of Chemistry

Committee on Final Examination

_____

Vladimir Katovic, Ph.D.

_____

David A. Grossie, Ph.D.

_____

Suzanne K. Lunsford, Ph.D.

_____

Andrew Hsu, Ph.D.
Dean, Graduate School.

ABSTRACT

Frock, Lynn R. M.S., Department of Chemistry, Wright State University, 2012. Synthesis and Electrodeposition of Mixed Metal Trinuclear Clusters of Molybdenum and Chromium in Ionic Liquid onto a Platinum Electrode

Electrochemical properties of $[Mo_3O_2(O_2CCH_3)_6(H_2O)(CF_3SO_2H)_2$ and $[Cr_2Mo(u_2\text{-}CH_3COO)_6(u_3\text{-}O)(H_2O)_3]$[CF3SO3] in 1-ethyl-3-methylimidazolium bis(pentafluoroethanesulfonyl)-imide ionic liquid was investigated. Cyclic voltammograms using a Platinum electrode indicated deposition had occurred for the $[Mo_3O_2(O_2CCH_3)_6(H_2O)(CF_3SO_2H)_2$ metal cluster but had not for the polynuclear complex $[Cr_2Mo(u_2\text{-}CH_3COO)_6(u_3\text{-}O)(H_2O)_3]$[CF3SO3]. Constant potential electrolysis of -1.23 V using a platinum foil electrode was performed. Scanning electron microscopy in combination with energy dispersion spectroscopy confirmed that deposition had occurred.

TABLE OF CONTENTS

TABLE OF CONTENTS (CONTINUED)

LIST OF FIGURES FIGURE

PAGE

LIST OF FIGURES (CONTINUED)

LIST OF FIGURES (CONTINUED)

LIST OF TABLES

TABLE PAGE

ACKNOWLEDGEMENT

I would like to express my most earnest of gratitude to Dr. Vladimir Katovic, my research advisor during the duration of my graduate work. His advice, patients and encouragement, throughout my research project has been the key to my success in completing my degree. The values he has instilled in me will remain with me for the rest of my life.

I would also like to thank my committee members, Dr. David Grossie and Dr. Suzanne Lunsford for their guidance, wisdom and assistance. Thank you for always taking the time to discuss the details of my project.

I would like to thank my fellow research students especially Linda Ubadigbo for giving me advice, clarification and always helping me if I needed it. You have been a wonderful friend. I would also like to thank Brandon Yocum, Markeata Lee, Tahiru Sulley and Denis Lennarts for all their support thought out my time in the graduate program.

I would like to thank my parents for all their love, support and for teaching me the values of diligence and integrity.

I would like to thank my husband who has made many sacrifices in order for me to receive my degree. I love you dearly.

DEDICATION

To the four strongest women in my life, my mother Myra kegley, my two former supervisors, Donna Brandelik and Michelle Harris and my best friend of thirty years, Rebecca Sparks. You all have been a huge part in my journey through life and have given me inspiration, wisdom and courage in knowing I can do anything I set my mind to do. Thank you from the bottom of my heart. In a collective effort you have made me the woman I am today.

I. INTRODUCTION

MOLTEN SALTS

A molten salt is a liquid obtained by melting an inorganic salt at extremely elevated temperatures. An example of a molten salt is sodium chloride (NaCl), that melts close to 800^0C (1474^0F)[1]. Molten salt mixtures are used in a variety of ways. For example molten chloride salt mixtures are commonly used in the process of alloy heat treatments. Molten salts are also used in the electrolytic production of metals such as uranium and aluminum. They have desirable characteristics such as good ionic conductivity, chemical and heat transfer properties. They are generally stable at very high temperatures and have relatively low vapor pressures.[2] Molten salts do have several undesirable characteristics which include corrosiveness and difficulty in characterizing. They tend to be hydroscopic and attract water molecules from the surrounding environment. Their high melting points make them extremely dangerous to work with and require extra safety precautions to be taken when handled.

IONIC LIQUIDS

Ionic liquids are quite similar to molten salts. Researchers in the 1960's found that by mixing inorganic and organic salts the melting point of the salt mixture could be

greatly reduced.[3] The mixture is composed of a bulky organic cation and a smaller inorganic anion.[4] Ionic liquids are salts that are liquids at ambient temperatures and contain strong ion-ion interactions that are not prevalent in molten salts.[5] This strong ion-ion interaction gives rise to some very interesting physical and chemical properties such as a large electrochemical window with a difference of approximately 4.0 volts between the cathodic and anodic decomposition potential. Most do not react with air and are not hydroscopic. They are stable at ambient temperature and have much lower melting points. They also have low vapor pressures, low densities, low dielectric constants and a wide range of thermochemical and electrochemical stability. Additionally they also have properties that make them useful as solvents in a variety of chemical applications due to their high conductivity and non-corrosiveness. Also, they are less toxic and safer to work with overall. Ionic liquids can be modified by to suit a particular application by choosing different anions or cations in the salt mixture[5,6]. Choosing which anion to use is critical in designing the most suitable ionic liquid for a given application. The physical properties of ionic liquids can be altered by changing the alkyl chain length of the anion[6]. For example, the anions BF_4^- and $CF_3SO_4^-$ are both air and water insensitive and thermally stable however, they give yield to ionic liquids with different physical properties because the potential window of an ionic liquid is increased as the alkyl chain length is increased. Substitution of the bulky cation also plays a role in the physical properties of ionic liquids. Using different cations can alter the ionic liquids melting point as well as the width of the electrochemical window.[6] Selection of the cation is critical due to the coulombic attraction between the cation and anion.[6] The study and synthesis of ionic liquids has grown exponentially since they were first discovered in the 1960's. The

synthesis of ionic liquids requires the reaction of a small inorganic anion, which governs the chemical properties of the liquid salt, with a bulky cation which determines the ionic liquids melting point.[7] Five of the commonly used cations used to synthesize ionic liquids are (a) Alkylsufonium, (b) Alkylphosphonium, (c) Alkyammonium, (d) N,N-alkylimidazolium, and (e) N-alkylpyridinium, shown in figure 1.

a.) $[SR_3]^+$ b.) $[PR_4]^+$ c.) $[NR_xH_{4-x}]^+$

d.) 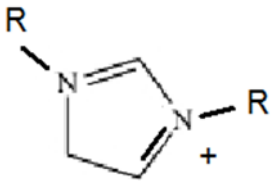

e.) 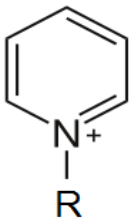

Figure 1. Five Commonly Used Cations in The Synthesis of Ionic Liquids

One of the most common cations used in the synthesis of ionic liquids is the 1,3-dialkylimidazolium cation[6] shown in figure 2.

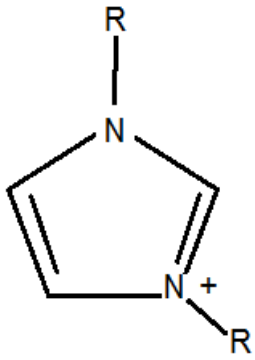

Figure 2. One of the most common cations used in the synthesis of ionic liquids 1,3-dialkylimidazolium cation

The 1,3-dialkyimidazolium salts are made up of dialkylimidazolium halides. The R is almost always a methyl group and R'can be varied to desired physical properties[7]. Table 1 is a list of cationic portions used to vary physical properties and table 2 lists some of the commonly used anions.

R' = Methyl MMImCl - $C_5H_9N_2Cl$
Ethyl EMImCl - $C_6H_{11}N_2Cl$
Propyl PMImCl - $C_7H_{13}N_2Cl$
Isopropyl iPMImCl - $C_7H_{13}N_2Cl$

Table 1. Cationic portions used to vary physical properties

Hexafluorophosphates - PF_6
Tetrafluoroborate - BF_4
Aluminate Halide - AlX_4 (X = [Cl, Br, or I]
Bis((pentfluoroethane)sulfonyl)imide – Beti

Table 2. Some of the commonly used anions

*anions are listed in order of increasing water solubility

Ionic liquids are currently being used in various processes such as batteries, metal electrodeposition, and photoelectrochemical cells.

METAL CLUSTER CHEMISTRY

In the early nineteen sixties F. A. Cotton used the term cluster to describe compounds containing metal-metal bonds.[8] The metal ion clusters contain at least two metal ions that are directly bonded together by a metal-metal bond. The transition metals of the second and third rows of the periodic table readily form very stable metal clusters due to their extended d-orbitals which favors overlap of valance orbitals.

One of the earliest examples of a metal cluster compound was the $[Mo_6Cl_8]^{4+}$ cation in which the Mo_6 is an octahedral cluster. In the octahedral metal cluster Mo_6, each triangle Mo_3 face is capped by a chlorine ion. The ligands for these and other types of clusters, for example O^{2-}, Cl^-, Br^- and I^- donate their π- electrons to the metals in the clusters center which optimizes the metal-metal bonding.[9]

Metal clusters are of interest due to their ability to act as a catalyst. There were not many compounds known with metal to metal bonds in the early nineteen sixties and since then there have been numerous transitional metal compounds that have been synthesized and characterized by X-ray crystallography and various types of spectroscopy.

Metal clusters are often referred to as transition metal cluster compounds and can be categorized either as early transitional metal clusters or late transitional metal clusters. There are two types of metal clusters; A). polynuclear carbonyls, nitrosyls, and similar related compounds; and B). halide and oxide complexes. Metal atoms of the type A have low formal oxidation states, -1 to +1, while those of type B are found in higher oxidation states, +2 to +3. Type A clusters are typically made up of late transitional metals, while type B clusters tend to consist of early transitional metals.[9]

Early transition metals

Early transition metals attributes include high stability, very strong M-ligand bonds, and are typically inert. The metal atoms they contain are in higher oxidation states and typically bond with Π-donor ligands [9]. The higher oxidation states helps to stabilize the metal cluster. The early transition metal homoleptic carbonyls have bond strengths that are stronger then late transition metals, as seen in Table 3.[26]

Compound	*D*, kj/mol	Compound	*D*, kj/mol
$Cr(CO)_6$	108	$Re(CO)_6$	192
$Mo(CO)_6$	152	$Fe(CO)_6$	117
$W(CO)_6$	178	$Co(CO)_6$	136
$Mn(CO)_6$	99	$Ni(CO)_6$	147

Table 3. Bond Strengths for Transition Metals

Early transition metals, also known as electron poor transition metal clusters or lower halides, are thought to contribute their excess electrons to the core metal due to contributions from their $\boldsymbol{\pi}$ - donor ligands, such as oxygen, chlorine, sulfur, bromine, iodine, and alkoxy molecules. The second and third transition metals specifically molybdenum, tungsten, tantalum and niobium have a formal oxidation state of +2 and +3. Maximum metal-metal bonding is achieved with higher oxidation states that help stabilize the metal cluster. Early transition metals strongly prefer to have a triangular and octahedral geometry. Figure 3 shows three examples of these geometries[13]

(1) triangular $[M_3X_9L_3]$ type e.g., $[Re_3Cl_{12}]^{3-}$ and (2) octahedral metal skeleton $[M_6X_8L_6]$ type e.g., $[Mo_6Cl_8L_6]^{4+}$ or (3) $[M_6X_{12}L_6]$ type e.g.,$[Nb_6Cl_{12}L_6]^{12+}$ (the chloro ligands bridge the 12 edges of the octahedron, L represents a suitable donor ligand)

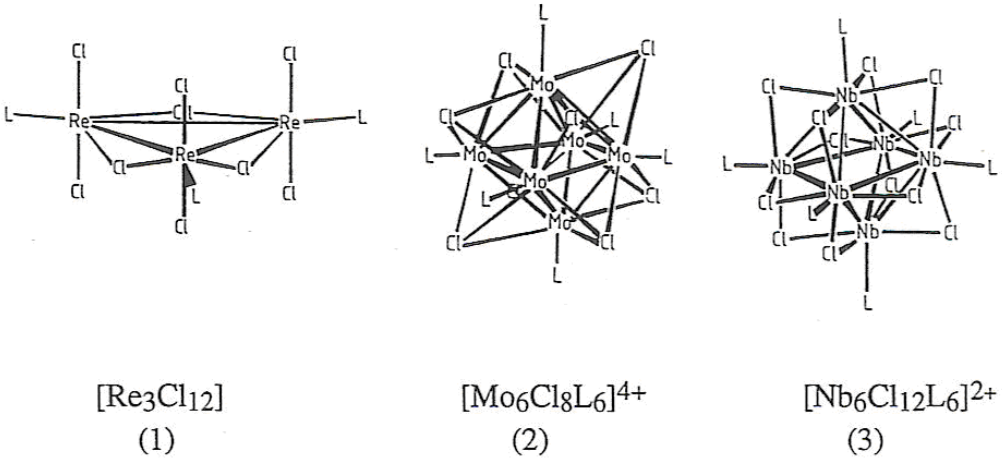

Figure 3. Octahedral and triangular geometries of Early Transition Metal clusters.

Late transition metals

The late transition metal clusters, sometimes referred to as electron rich transition metal clusters, contain metal centers such as, ruthenium, rhodium, and iridium in their low oxidation states. They are also typically known to contain carbonyl, nitrosyl, cyano, isocyanide, phosphine or hydido ligands. The carbonyl ligands are among the most common. The carbonyl ligand stabilizes the low oxidation state metal cluster by occupying the terminal, edge bridging or face capping positions of the cluster. These clusters contain **π-** acceptor ligands which due to their metal to ligand back-bonding, they

draw electrons from the metals. Late transition metals contain metals in low oxidization states, mostly zero, -1, or +1. They contain Π-acceptor ligands that withdraw electrons by Π-back-bonding. Late transition metals are highly reactive oxidizing agents that have weaker M-ligand bonds. Figure 4 shows an example of a late transition metal complex.

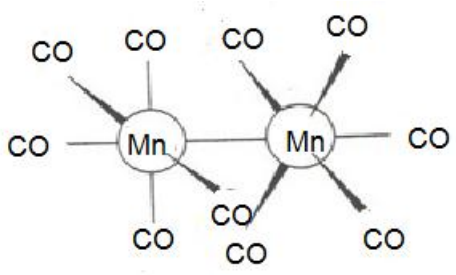

Figure 4. Late transition metal, $[Mn_2(CO)_{10}]$

The transitional metal clusters contain half filled d and s valence orbitals, therefore maximum binding energies occur at the center of the transition series. The ligands that surround the metal core attempt to modify the electronic configuration of the metal while also achieving maximum binding energy[10].

STRUCTURES OF TRANSITION METAL CLUSTERS

There are several different structural types of metal clusters, binuclear, trinuclear, tetranuclear , hexanuclear (octahedral) and Polynuclear metal complexes.

Binuclear Metal Clusters

Multiply bonded M-M dimmers with bond orders up to 4 are the most common binuclear metal cluster compound. $Re_2X_8^{2-}$ ions (X = Cl-, Br-) and binuclear carboxylates $M_2(O_2CR)_4$, (M = Cr, Mo, W, Re, or Ru) are well known examples of binuclear metal clusters. An example of a $Re_2Cl_8^{2-}$ is shown in figure 5.

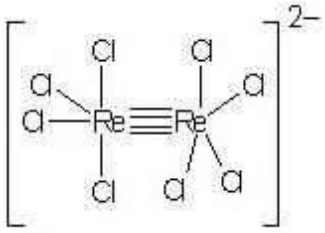

Figure 5. Structure of the Octachloridirhenate (III) ion The Re_2X_8

The $Re_2X_8^{2-}$ anion has two distinctive features; the first one is the extremely short distance between the two metal Re atoms being only 2.24 angstroms apart, compared to 2.75 angstroms in the rhenium metal and 2.48 angstroms in Re_3Cl_9. The other feature is the existence of the eclipsed configuration of the chlorine atoms in $Re_2Cl_8^{2-}$. The presence of the δ bond between Re atoms is proven by the eclipsed configuration of the chlorine atoms. This eclipsed configuration of the $Re_2Cl_8^{2-}$ ion was described by F. A. Cotton[8] and was central in proving that the quadruple δ did indeed exist between the Re atoms. Cotton was the first to describe the bonding of Re atoms in the dimer $Re_2Cl_8^{2-}$[7]. The Re atoms are joined along the z axis and each Re atom is bonded to four chlorine atoms. This geometry forms a square planar array. In each of the four Re-Cl bonds the dsp^2 hybrid orbitals are used (occupying the d_x^2-y^2orbital). The p_z and d_z^2 orbital lie directly along the Re-Re bond axis and are thought to be hybridized to form one orbital directed towards the other Re atom and another in the opposite direction. The orbitals of each Re atom overlap and form a sigma-bond (Figure 6-a). Each d_{xy} and d_{yz} orbital of Re are not perpendicular toward the other Re atom, which overlap to form the d-d π bonds. The resulting π bonds, one in the xz plane and one in the yz plane are shown in figure 6-

b. The forth metal-metal bond is able to form by the overlap of the two remaining d orbitals, $d_{xy,}$ of each Re atom. The sideways overlap of these d orbitals gives rise to the δ bond. This overlap can only exist if the chlorine atoms are in eclipsed form. The staggered form doesn't allow for the overlap of the d_{xy} orbitals and would result in no delta bonding.[10]

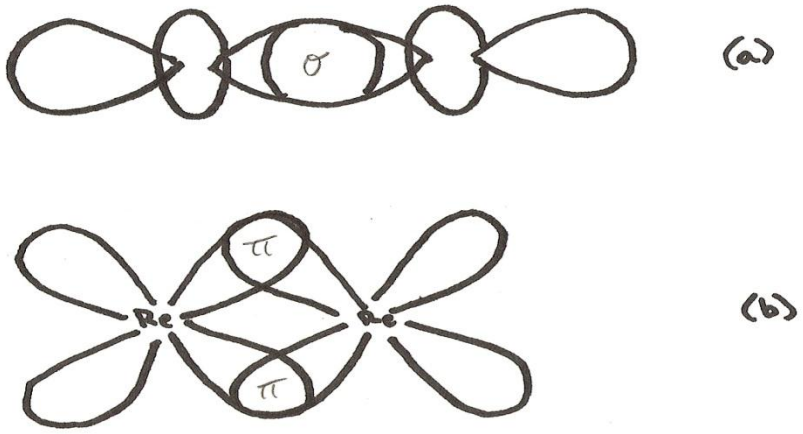

Figure 6. Multiple bonding between rhenium atoms, (a) Sigma bonding between Re atoms, (b) Two π bonds between Re atoms.[10]

There are four d electrons contributed from each Re atom allowing the formation of four bonds. The structure of the $M_2(O_2CR)_4$ dimer is shown in figure 7 (where M= Mo, W, Cr).[27]

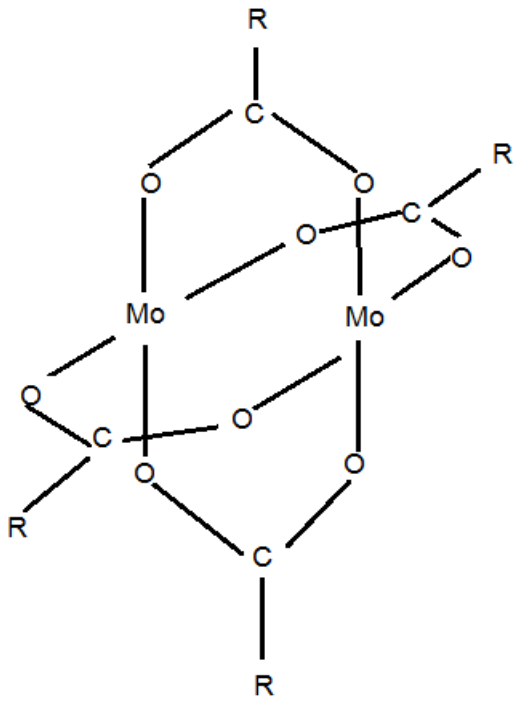

Figure 7. The structure of the the $M_2(O_2CR)_4$ dimer (where M= Mo, W, Cr).

The formal oxidation state of Mo in $Mo_2(O_2CR)_4$ is +2. The quadruply Mo dimers are easily oxidized by $1e^-$ to give rise to dimers with a bond order of 3.5.

$$Mo_2(O_2CR)_4 \ -e^- \rightarrow Mo_2(O_2CR)_4^{+} \ -e^- \rightarrow Mo_2(O_2CR)_4^{2+}$$

Trinuclear Metal Clusters

One of the best known examples of noncarbonyl clusters containing three metal atoms are the rhenium trihalides $[(ReCl_3)_3]$ and their derivatives. First discovered in 1932 by Geilnann, Wriuce, and Biltz[12], Each rhenium atom is bonded together both directly to the other by metal to metal bonds and indirectly by a bridging halogen ligand.

In addition each rhenium atom in the triangular geometry is coordinated by two or more

halide ligands below and above the plane defined by the three rhenium atoms (figure 8 a)[10]. The rhenium atoms of the diamagnetic Re_3Cl_8 cluster are bridged by halide ions with adjacent Re_3Cl_8 clusters which gives rise to a polymeric structure[11] (figure 8 b). A dodecahalotrirhenate(III) ion $Re_3X_{12}^{3-}$ is produced when Re_3X_8 is dissolved in a hydrochloric acid solution (figure 8 c)[11]. The behavior of other halides is the same as Cl.

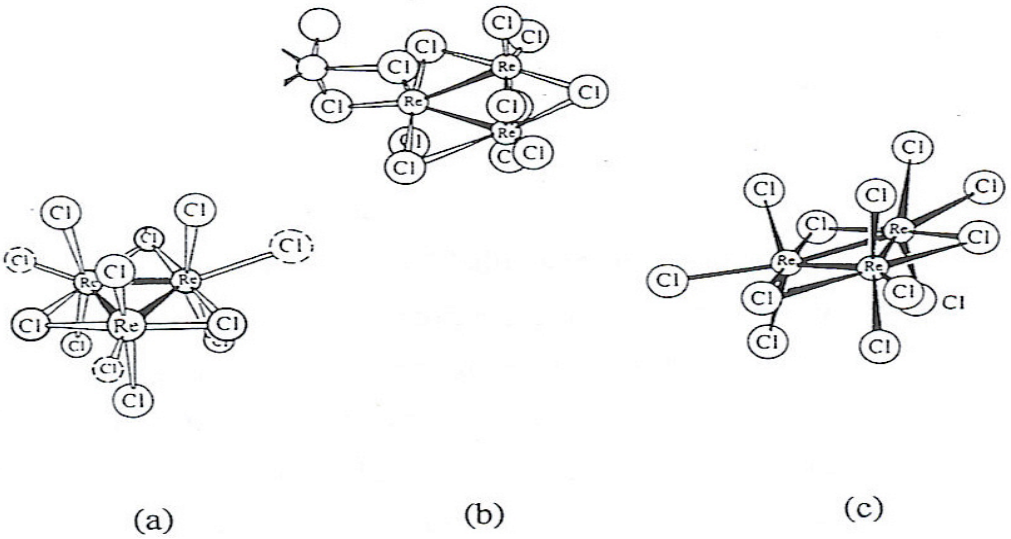

Figure 8. Structures of trinuclear rhenium metal clusters, (a) Re_3X_9, (b) polymeric structure of Re_3X_8, (c) $Re_3Cl_{12}^{3-}$

Trinuclear triply-bonded compounds of the type M_3X_6 constitute an important and extensive area of chemistry.[14] Trinuclear metal clusters with bond orders between 2/3 and 1 are generally formed by the early transition metals in their lower oxidation states such as molybdenum, tungsten, niobium, and titanium. Their geometry is a triangular M_3 unit. The basic structures of this type of clusters are known as; (M_3X_6 type), without μ3-ligands (figure 9) is given by the cluster $[M_3X_6 (C_6Me_6)_3]^{n+}$ where M = Nb, Ti, Ta and X = Cl, or Br. The three metal atoms have direct metal-metal bonds to each other and are

surrounded by four chloride ligands in a square planar formation with three C_6Me_6 molecules coordinating on the axial plane. The second type (M_3X_{13} type), with one μ3-ligand (figure 10) M_3X_{13} structure type is given by the formula $[M_3(\mu 3\text{-}X)(\mu\text{-}Y)_3L_9)]$ where M = Ti, Nb, Mo, and W. X= μ3 capping ligands can be Cl^-, Br^-, I^-, O_2^-, $OCH_2CMe_3^-$, and S_2^-. Y = μ2 bridging ligands can be Cl^-, Br^-, I^-, O_2, S_2^-. The terminal ligands L can be OEt^-, O_2CCME_3, CN^-, H_20, and the halide ions. The third type (M_3X_{17} type), with two μ3-ligands, M_3X_{17} structure (figure 11) with two ligands is given by formula $[M_3(\mu_3\text{-}X)_2(\mu\text{-}O_2Y)_6L_3)]$. The metals are Mo and W while the X can be O_2^- or OEt^-. The bridging bidentate ligands O_2Y can be $MeCO_2$, $EtCO_2$, $tBuCO_2$ and monodentate ligands L can be, $MeCO_2$, $tBuCO_2$ and H_20.

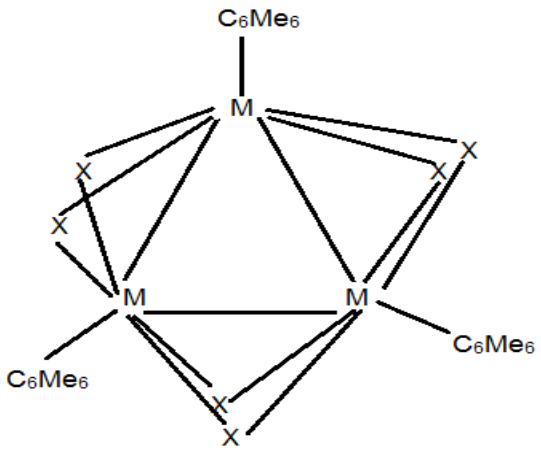

Figure 9. Structure type (a) $[M_3X_6(C_6Me_6)_3]^{n+}$ (no μ_3 ligand)

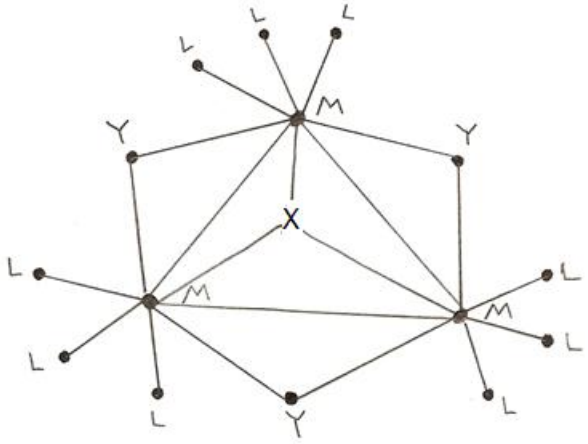

Figure 10. Structure type (b) $[M_3(\mu_3\text{-}X)(\mu\text{-}Y)_3L_9)]$ (one μ_3 ligand)

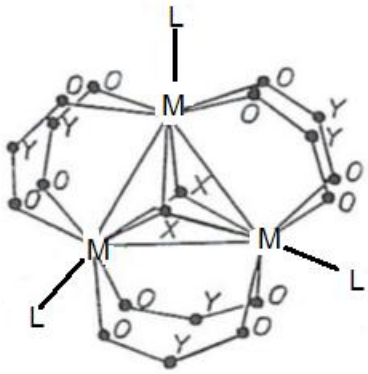

Figure 11. Structure type (c) $[M_3(\mu_3\text{-}X)_2(\mu\text{-}O_2Y)_6L_3)]$ (two μ_3-ligands)[12]

Tetranuclear metal clusters

Tetranuclear metal clusters are very uncommon, however they can be formed by the dimerazation of quadruply bonded binuclear compounds. This dimerization will give rise to a planar structure, a tetrameric structure. There are very few examples of a tetrahedral structure metal clusters found that contain carbonyl ligands.[12] Figure 11 shows an example of a quadruply bonded binuclear compound as a result of dimerization.

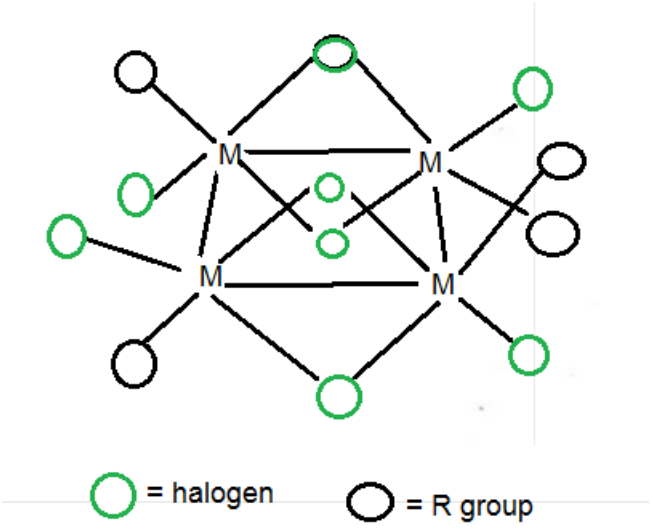

Figure 12. Quadruply bonded binuclear compound as a result of dimerization[12]

Hexanuclear Metal Clusters

Hexanuclear metal clusters are clusters that contain six metal atoms. Some of the earliest Hexanuclear clusters synthesized contained molybdenum, niobium, or tantalum atoms. These types of clusters can be formed by having either single bonds to several other metal atoms or by having multiple metal-metal atom bonds. This is a result of the low oxidation state of the metal. There are two types of hexanuclear clusters;

1. The metal atoms form an octahedral cluster configuration with eight ligands bridging three of the six metal atoms. The ligands are positioned above the triangular faces of the octahedron.

2. This type has the same core structure but has 12 ligands with each bridging two metal atoms.

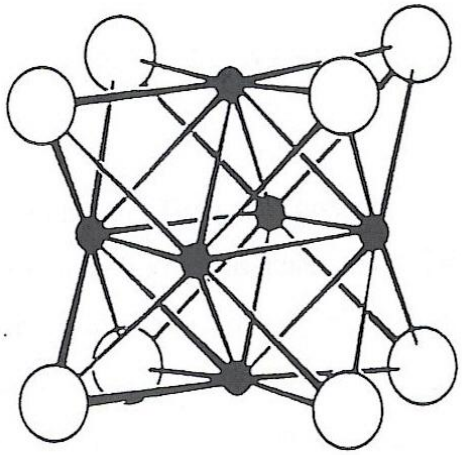

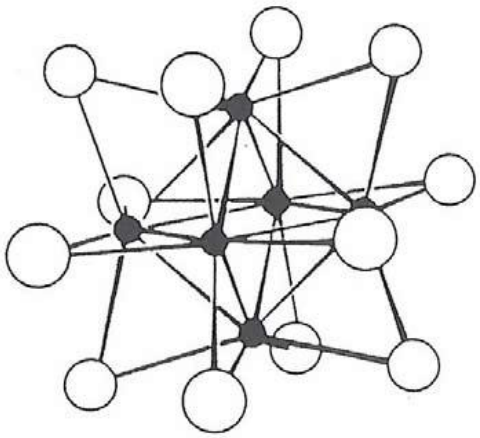

$[Mo_6Cl_8]^{4+}$ $[M_6 X_{12}]^{2+}$ where X= Cl, Br

Figure13. Examples of hexanuclear structure types.[13]

Polynuclear metal complexes

Polynuclear metal complexes are inorganic complexes that contain two or more metals that do not have direct metal-metal bonds. Metal atoms in these compounds are stabilized by bridging ligands. In some cases of mixed metal polynuclear complexes the metals have been shown to exhibit covalent bonding of certain metals. Some common inorganic bridging ligands are: CO, OH^-, SH^-, and NH_2^-. Figure 14 shows an example of the Polynuclear complex, $Cr_3O(CH_3CO_2)_6(H_2O)_3^+$.

Figure14. Polynuclear complex, $Cr_3O(CH_3CO_2)_6(H_2O)_3^+$

METAL CLUSTER COMPOUNDS AS CATALYST

Metal cluster compounds are considered to be good candidates for improved catalyst. In 1836 Jöns Jakob Berzelius [14] was said to have coined the term catalyst to refer to the chemical reactions that are accelerated by substances that remain unchanged after the reaction has taken place. Transition metals and their compounds are now well known for their homogeneous and heterogeneous catalytic activity. This activity is due to their ability to adopt multiple oxidation states and to form different types of complexes[9]. Catalysts at a solid surface, such as an electrode, involve the formation of bonds between reactant molecules and the atoms at the surface of the catalyst. Both early and late transition metals utilize 3d and 4s electrons for bonding which has the effect of increasing the concentration of the reactants at the catalyst surface and also weakening of the bonds in the reacting molecules by lowering the activation energy needed to break bonds. The transition metal ions have the ability to change their oxidation states which makes them effective as catalysts. In metal cluster compounds each metal atom is directly bonded to an adjacent metal atom, but in metal cluster compounds the bonds are much shorter then

in homogeneous metals. There are several advantages of metal cluster compound catalyst over traditional mononuclear catalyst. The properties of metal cluster compounds can be altered by changing the type of ligands, the structural configuration and by incorporating different metals into the cluster. They are soluble in an array of common solvents. They have the ability to bind to very small molecules through multiple metal ligand bonds. Due to these abilities metal clusters should work well as catalyst for the reduction of small molecules such as CO, N_2, and O_2. An example being the hydrogenation of carbon monoxide cannot be catalyzed by mononuclear metal catalyst,[16] however the metal cluster compounds have been shown to catalyze the reduction[17] of CO to CH_4 and H_2O.

ELECTROCHEMICAL METHODS

Electrochemical methods provide efficient and straightforward assessment of the redox behavior of molecular systems. The most common electrochemical method used by chemist today is the voltammetric or potential sweep method. Voltammetry is a correlation between applied potential and current. In all potential sweep methods, the potential (V) of the working electrode is varied continuously with time according to a predetermined potential waveform or excitation function, while the current (I) is concurrently measured as a function of the potential. The applied potential at the working electrode is measured against a reference electrode of choice, while a counter electrode or auxiliary is required to balance the I-V applied. Thus, three electrodes are required, a working electrode, a reference electrode and an auxiliary electrode. An electrolyte salt must also be dissolved in solution to maintain sufficient conductivity in the bulk solution. Common types of working electrodes include glassy carbon, platinum, silver and gold.

Common types of auxiliary electrodes include Pt wire, and glassy carbon rods. Common types of reference electrodes include Ag/AgCl, Normal hydrogen electrode (NHE), saturated calomel electrode and Ag/Ag/NO_3. Figure 15 shows a typical electrochemical cell used for potential sweep voltammetry.

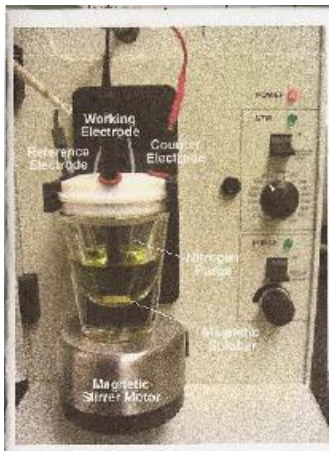

Figure15. Typical electrochemical cell used for potential sweep voltammetry.

Linear Sweep Voltammetry

Linear sweep voltammetry (LSV) is the most basic potential sweep method. In LSV the potential of the working electrode is varied linearly with time between two values for example, the initial (E_i) and final (E_f) potentials. While the electrode potential is steadily increasing or decreasing during the experiment, a level of ohmic current flows continuously. The currents are due to the capacitive charging of the working electrodes double layer or Helmholtz layer. When the potential reaches a value in which the chemical species in the solution undergo electrochemical conversions Faradaic current will also flow. Figure 15 shows bulk solution when no potential is applied. Figure 16

shows that as potential is applied ohmic current begins to flow. Figure 17 shows the formation of the Helmholtz double layer in the electrochemical cell.[32]

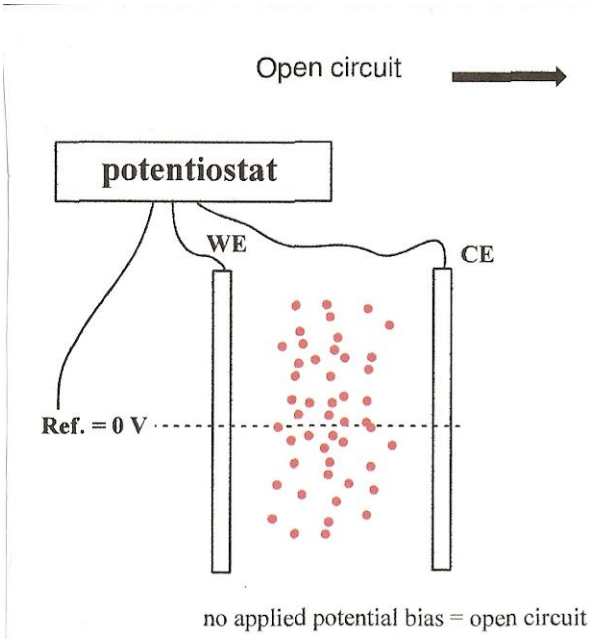

Figure16. Bulk solution as no potential applied.[32]

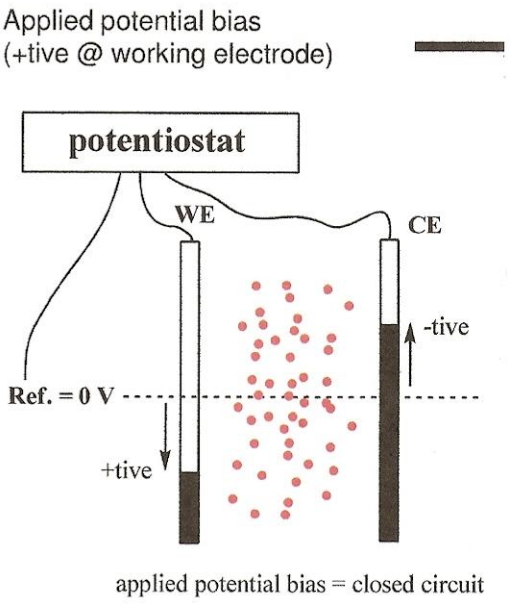

Figure17. Potential applied [32]

(Figure reproduced with permission from Taylor & Francis Group LLC- Books)

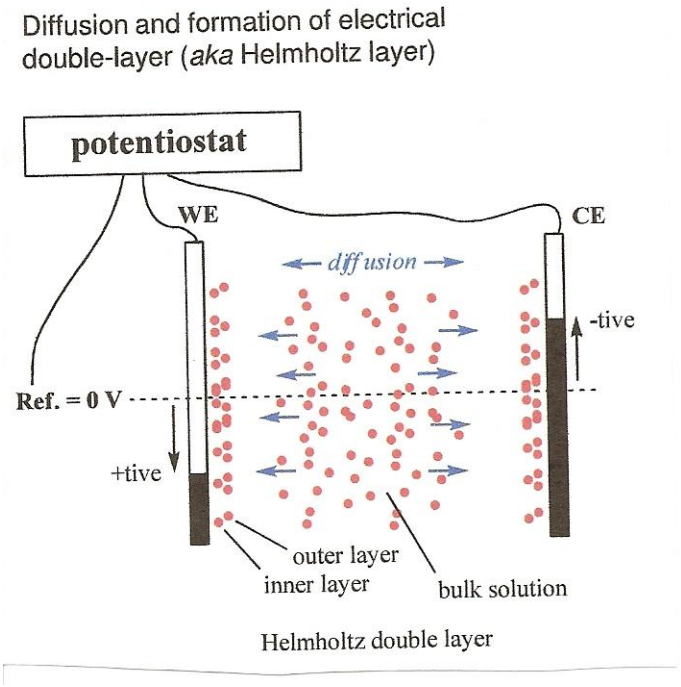

Figure18. Formation of the Helmholtz double layer in the electrochemical cell.[28]

(Figure reproduced with permission from Taylor & Francis Group LLC- Books)

Relative to the bulk solution redox chemical reactions only occur in the electrical double layer.[32]

Cyclic Voltammetry

Cyclic voltammetry (CV) is similar to linear sweep voltammetry. It is based on the same fundamental principles however, in cyclic voltammetry the potential of the

working electrode is varied linearly with time between three values, $E_i \rightarrow E_{sp} \rightarrow E_f$. In CV the potential of the working electrode is scanned back after reaching a chosen value, the switching potential (E_{sp}). During the forward scan or reduction sweep, the E_i is more positive than the E_f and the current is a result of the reduction of species. After reaching E_{sp} the reverse scan begins and the anodic current is a result of the re-oxidation of the previously reduced species. Figure 18 shows the excitation function for a LSV experiment and figure 19 shows the excitation function for a CV experiment.[28]

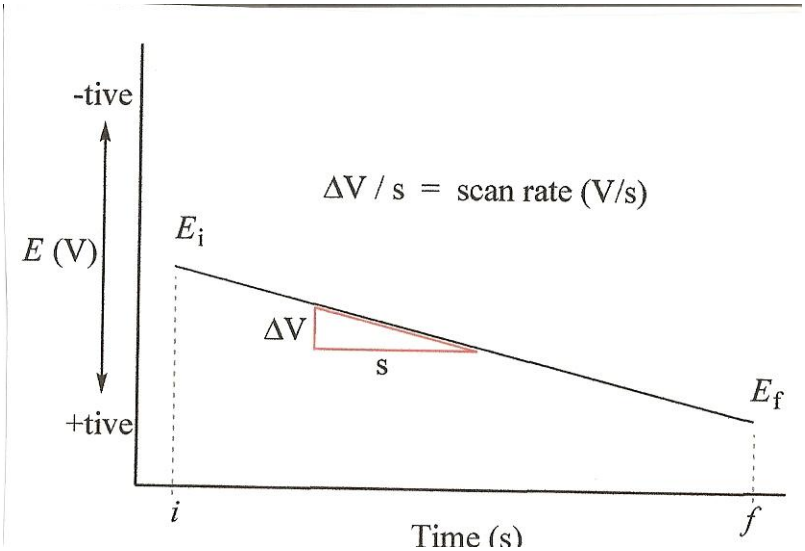

Figure19. The excitation function for a LSV experiment.[32]

(Figure reproduced with permission from Taylor & Francis Group LLC- Books)

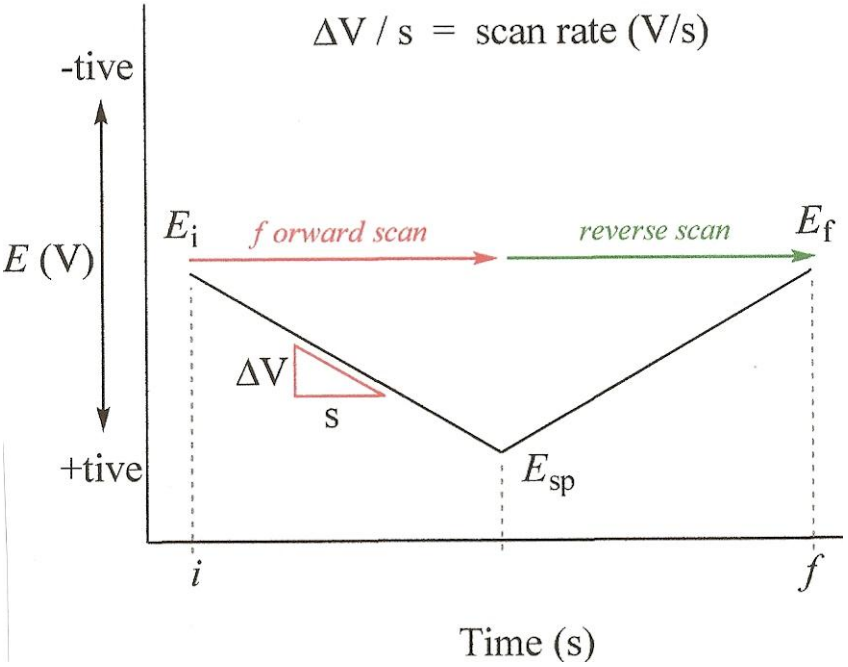

Figure20. The excitation function for a CV experiment.[32]

(Figure reproduced with permission from Taylor & Francis Group LLC- Books)

Cyclic voltammetry can be used to study the redox properties of a large variety of organic and inorganic chemical species. Modern instruments allow the experimentalist to choose multiple switching potentials in order to carry out tailored CV scans over a chosen potential window which allows for rapid location of redox potentials as well as the kinetics of heterogeneous electron transfer reactions. It is also a simple method to analyze the electrolyte solutions effect on the overall redox reaction. The potentials at which the maximum peak currents occur are called E_p values. The potentials for the oxidizing anodic and reducing cathodic sweep directions are referred to as E_{pa} and E_{pc} respectively. If the scan rate is varied and the effect on the relative magnitude of both the

anodic current I_{pa}, and the cathodic current $I_{pc,}$ are determined, the rate constants for decomposition of the process can be deduced. The potential $E_{1/2}$ for an electrical process is determined by $(E_{pa} + E_{pc}) / 2$. The value of $E_{1/2}$ corresponds to the redox potential of the complex provided the diffusion properties of both the reduced and oxidized species are very similar. In an ideal redox process $\Delta E_p = |E_{pa} - E_{pc}| = 0.059$ V for an one electron redox reaction process. The characteristic half wave potential $E_{1/2}$ of a redox couple is usually within a few mV of the formal potential E^o for the couple according to the Nernst equation shown below.[28]

$$\mathbf{E_{1/2} = E^0 - (RT/2nF)\ ln(D_{ox}/D_{red})}$$

The ratio of the diffusion coefficients D_{ox} and D_{red} is usually close to unity. The ease of determining half wave potentials and close approximation of formal potentials makes CV an attractive method in the study of redox processes.

It is common to determine the reversibility of a redox reaction by comparing ΔE_p values of an unknown complex to the values of reference know complex. Ferrocene, $Fe(C_5H_5)_2$ is commonly used as a reference complex in redox studies. Figure 21 shows the reversible redox reaction of ferrocene $(n^5\text{-}C_5H_5)_2Fe^{2+}$ → ferricenium $(n^5\text{-}C_5H_5)_2Fe^{3+}$.

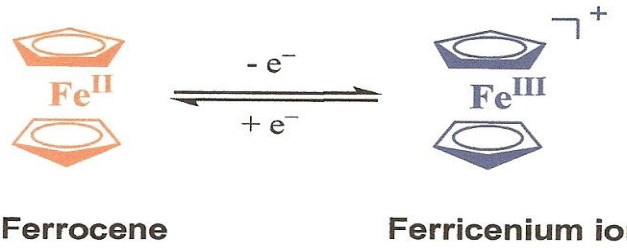

(Figure reproduced with permission from Taylor & Francis Group LLC- Books)

Figure 21. Reversible redox reaction of ferrocene → ferricenium[28]

$(n^5\text{-}C_5H_5)_2Fe^{2+} \rightarrow (n^5\text{-}C_5H_5)_2Fe^{3+}$

Figure 22 shows a cyclic voltammagram for a reversible one electron redox couple of $Fe(C_5H_5)_2$ in acetonitrile against an Ag/AgCl reference electrode with $E_{1/2}$ = 0 V.[28]

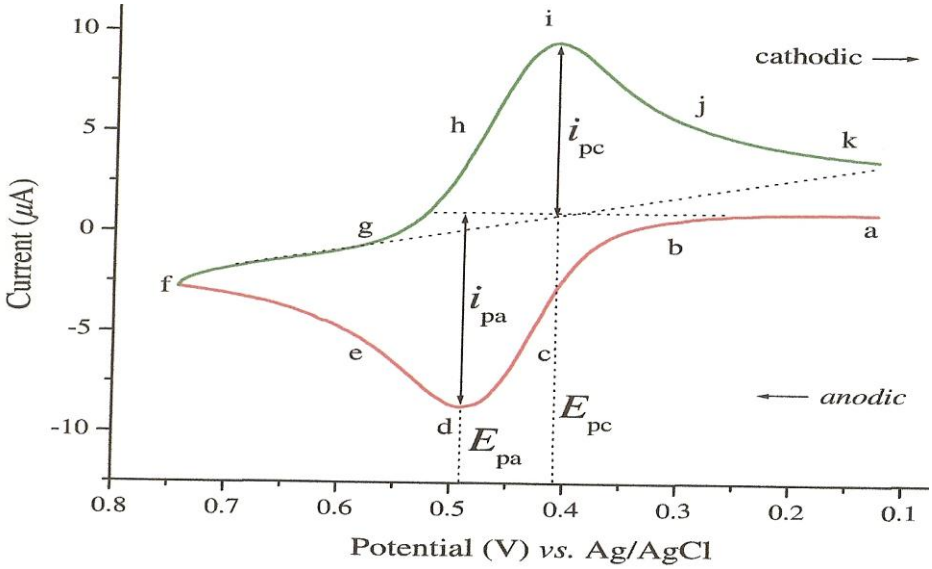

Figure 22. Cyclic voltammagram of a reversible Fe $^{+3/+2}$ $1e^-$ redox couple, $E_{1/2}$ = 0V [32]

(Figure reproduced with permission from Taylor & Francis Group LLC- Books)

a. Initial potential at 0.10 shows no current, thus no electrolysis when electrode is turned on.
b. Electrode scanned in a more positive direction.
c. Potential is made more positive and electrode is now a strong oxidant to oxidize ferrocene $(n^5\text{-}C_5H_5)_2Fe^{2+}$ to ferricenium $(n^5\text{-}C_5H_5)_2Fe^{3+}$.

d. As anodic current increases the concentration of ferrocene decreases rapidly at the electrode surface causing the current to peak.

e. Current decays as ferricenium surrounds the electrode and ferrocene concentration is depleted.

f. Scan is now reversed at the switching potential E_{sp} of 0.75 V In between points f and g anodic current continues as potential is sufficiently positive to oxidize ferrocene.

g. At point h the electrode is now a strong reductant able to reduce the ferricenium that has accumulated adjacent to the electrode surface and the reversible redox reaction of ferricenium $(\eta^5\text{-}C_5H_5)_2Fe^{3+} \rightarrow$ ferrocene $(\eta^5\text{-}C_5H_5)_2Fe^{2+}$ takes place.

Cyclic voltammetry can provide four important parameters of a redox process, the anodic peak current, I_{pa}, the cathodic peak current, I_{pc}, the anodic peak potential, E_{pa}, and the cathodic peak potential E_{pc}. These four values can be used to determine the number of transferred electrons, n, the heterogeneous rate constant K_n and the standard reduction potential E^o. If the redox process is electrochemically reversible a characteristic cathodic wave is observed with a maximum current value given by the Randles-Sevcik equation shown below.[28]

$$I_p = [(2.69x10^5)\, n^{2/3}\, A(D_{ox}v)^{1/2}C_{ox}\Psi]/[RT]^{1/2}$$

I_p= peak current; n = number of electrons; A= working electrode area (cm^2); C = analyte concentration (m/cm^3); v= potential scan rate (V/s) D = diffusion coefficient (cm^2/s). [32]

The three types of systems that are prevalent in cyclic voltammetry are a reversible system, a quasi-reversible system, and an irreversible system. The type of system depends on the rate constant of the process. Slow electron exchange (very small K^0) during the redox process will cause the system to be irreversible. If the current from the reverse sweep is not displayed in a CV scan then a system is irreversible. If the peak potential separation is greater than 59.2 V than the system is quasi-reversible and will increase with increased scan rate. Figure 23 depicts the difference between the reversible system and the quasi reversible system. A quasi reversible system is caused by the magnitude of the electron exchange rate being similar to that of the cyclic voltammetry. In an irreversible system the current on the reverse sweep will not show up.

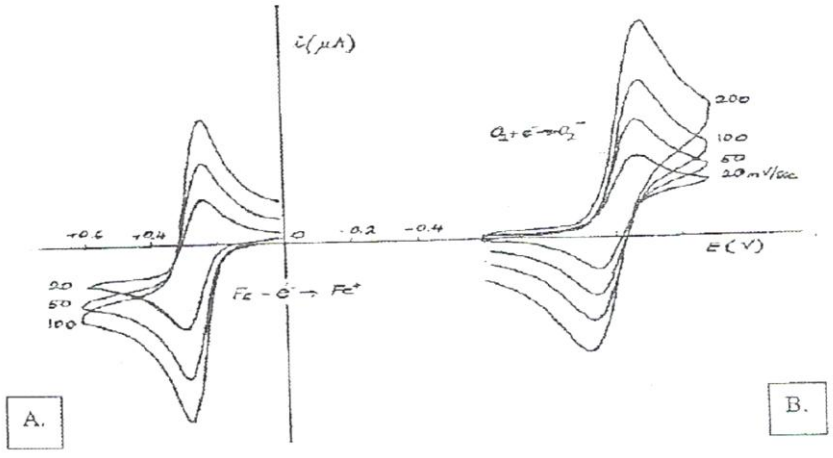

Figure 23. Cyclic voltammagrams of: A. Reversible system and B. Quasi reversible system.[23]

II. EXPERIMENTAL

Materials

The following materials were purchased from Alfa Aesar company: Acetic Anhydride (97+%) Trifluoroacetic acid (99%), Trifluoromethanesulfonic acid (98+%), Hexacarbonyltungsten (97%), and Dowex 50wx2 100-200 (H). Molybdenum hexacarbonyl technical grade was purchased from Fluka Chemical Company. Sodium tungstate dehydrate (99%) , and Chromium(II) acetate dimer monohydrate was purchased Aldrich Chemical Company. Acetonitrile, gradient grade +99.0% and triethylamine was purchased from Fisher Scientific and used as received. Trifluoromethanesulfonic acid (99.5%) was obtained from Alfa Aesar.

Instrumentation

UV-VIS electronic absorption spectra were obtained using an Ocean Optics 4000 spectrophotometer interfaced with an Apple computer and a HP 8100 printer. The UV-Vis scans of samples were taken using ionic liquid or water as a solvent blank in 1-cm quartz cell. IR spectra were obtained from a Themo Scientific Nicolet 6700 FTIR interfaced with a Dell computer and a HP printer. Crystallography data was obtained

using a Bruker/Mitigen sample mount and ran in a Smart X2S Bruker/Mitigen instrument.[30] Crystallography data was analyzed with Apex 2 and Oscail software.[31] The amount of water in the ionic liquid was determined using a Denver Instrument Coulometric Karl Fisher Titrator interfaced with a Model 260 titrator controller. Approximately 20 microliters of liquid was injected into the titrator using a stainless steel needle and a glass syringe. The syringe was washed in ethanol and the dried in an oven with temperatures from 60 to 80 degrees Celsius between uses. Cyclic Voltammetry experiments were performed using an EG+G Princeton applied Research (PAR) 173 Potentiostat/Galvanostat System with a PAR 75 universal Programmer. A MacLab/4 analog digital converter was used to convert analog data recorded using Scope V3 software. Scanning electron microscopy was performed on a FEI Quanta SEM equipped with an Electron energy dispersion scope.

The cyclic voltammograms were obtained using a platinum disk working electrode, an Ag/AgCl reference electrode, and a platinum auxiliary electrode. The platinum disc electrodes (1mm) were obtained from Cypress Systems Inc. The cell volume ranged from 0.5mm to 1ml. The electrochemical cell is shown in Figure 24.

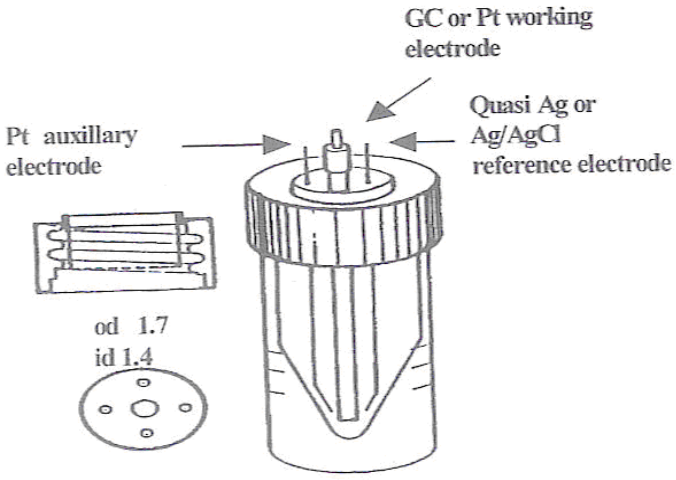

Figure 24. Example of electrochemical cell

Preparation of 1-ETHYL-3-METHYLIMIDAZOLIUM Bis(pentafluoroethane sulfonyl)

The ionic liquid 1-ETHYL-3-METHYLIMIDAZOLIUM Bis(pentafluoroethane sulfonyl) imide was previously synthesized and identified.[19] Water was removed from the sample by placing on high vacuum with a liquid nitrogen trap for several days. CV scans indicated the presence of chlorine ions. Chlorine ions were removed by repeated washes with 40 ml of H_2O followed by fine frit filtering and then placed back on high vacuum for several days.

SYNTHESIS OF METAL CLUSTERS

The formation of the metal-metal quadruple bond in the acetate derivative of molybdenum (II) carboxylate compounds presented the challenge of creating an air free environment to prevent the oxidation of the compound and intermediates. The binuclear metal dimer of molybdenum tetracarboxylate , $Mo_2(O_2CR)_4$ and the metal Chromium

tetracarboxylate dimer ,$Cr_2(O_2CR)_4$, were prepared and handled under a nitrogen purge utilizing the Schlenk technique. Synthesis of the trinuclear metal clusters were all done under a nitrogen purge to prevent the air oxidation of the reactants.[20,27]

Synthesis of $Mo_2(O_2CCH_3)_4$ - tetra (acetato) dimolybdenum (II)

$MO_2(O_2CCH_3)_4$ was synthesized by heating the triply bonded +3 dimer of $2Mo(CO)_6$ in solution with a stoichiometric amount of acetic acid. The process strips CO ligands from $Mo(CO)_6$ and allows for the oxidation of Mo atoms by the acetic acid.[20] The resulting product is the quadruply bonded +2 dimer $MO_2(O_2CCH_3)_4$.[27] The extremely air sensitive dimer product was filtered in a glove box under N_2 purge using a schlenk filter. The final product was stored in sealed vials and left in N_2 purged desiccator containing Phosphorous pentoxide (P_2O_5) for later use.

$$Mo_2(CO)_6 + 4HO_2CCH_3 \text{----}\rightarrow Mo_2(O_2CCH_3)_4 + 12CO + H_2$$

Synthesis of $[Mo_3O_2(O_2CCH_3)_6(H_2O)_3](F_3CCOOH)$ – Hexa-μ_2-acetato-di- μ_3-oxo-tris(aqua-molybdenum (IV)- trifluoromethylacetate

This synthesis was accomplished by finely grinding 1.21 g (5.0 mmol) of Na_2MoO_4 and placing into a 200 ml schlenk flask which contained a mixture of 70 ml of acetic acid, I ml of triethyl amine and 7 ml of acetic anhydride. The mixture was deareated with N_2 and placed under heat with a constant N_2 purge. The mixture was allowed to reflux for 30 minutes after which 12.0 g (2.0 mmol) of $Mo_2(O_2CCH_3)_4$ was quickly added. The

mixture was refluxed for 72 hours while stirring under a N_2 purge. A color change was to dark brown observed when all the solids had dissolved. After refluxing the solution was allowed to cool to room temperature and diluted with 200 ml of H_2O. The diluted mixture was then filtered. The filtrate was then poured into a Dowex 50x2-200 cation exchange resin column previously prepared with HCl. After rinsing the column with H_2O the filtrate was slowly eluted using 1.0M Trifluoromethyl acetic acid. Four layers were developed in the column from top to bottom, one blue green, one dark blue, one yellow and one light pink. The solution was, then, evaporated on the rotatory evaporation system at 80 ^oC under vacuum to remove the excess H_2O. The remaining eluent was allowed to slowly evaporate and produced dark red crystals of the product $[Mo_3O_2(O_2CCH_3)_6(H_2O)(CF_3CO_2H)_2$.[20,27]

Synthesis of $Cr_2(O_2CCH_3)_4$

An aqueous solution of a Cr^{3+} compound is first reduced to the chromous state using zinc according to the following reaction.[20]

$$2Cr^{3+} + Zn \rightarrow 2Cr^{2+} + Zn^{2+}$$

The resulting blue product is then treated with sodium acetate which results in the rapid participation of chromous acetate as a bright red powder according to the following reaction.[20]

$$2Cr^{2+} + 4OAc + 2H_2O \rightarrow Cr_2(OAc)_4(H_2O)_2$$

Any introduction of air into the apparatus is indicated by a discoloration of the bright red product.[21] Figure 25 shows the structure of a $Cr_2(OAc)_4(H_2O)_2$ molecule.

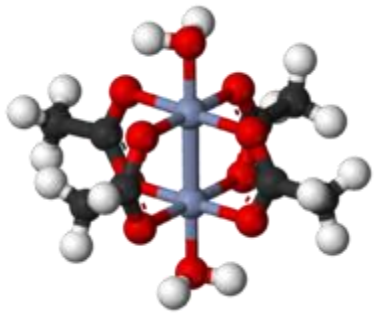

Figure 25. Structure of a $Cr_2(OAc)_4(H_2O)_2$ molecule

The red colored compound of $Cr_2(OAc)_4(H_2O)_2$, like that of $Mo_2(OAc)_4$, contains a quadruple bond between the two metal atoms. The molecule contains two chromium atoms, four monoanionic acetate ligands and two ligated molecules of water. The coordination environment surrounding each chromium atoms consists of a total of four oxygen atoms coming from each acetate ligand, one water molecule in the axial position and the second chromium atom being opposite of the water molecule. This environment gives the chromium center an octahedral geometry. The molecule has D_{4h} symmetry. The same structure as a molecule of the Molybdenum(II) acetate dimer. The main difference between the two structures are the reported bond lengths between each molecules central metal atoms, with Mo-Mo reported as 2.093Å and Cr-Cr reported as 2.36 Å[10]. The quadruple bond found between the two chromium atoms arises from the overlap of its four d- orbitals of each metal atom with the same orbitals of the other metal atom. The sigma bond comes from the overlap of the z^2 orbitals and the overlapping orbitals of the

xz and yz gives rise to two pi bonds. The fourth bond, the delta bond is from the xy orbitals overlapping. Because the Cr is in a 2+ oxidation state it is a good reducing agent. The formation of the quadruple bonds on the two Cr atoms is shown in the MO diagram in figure 26.

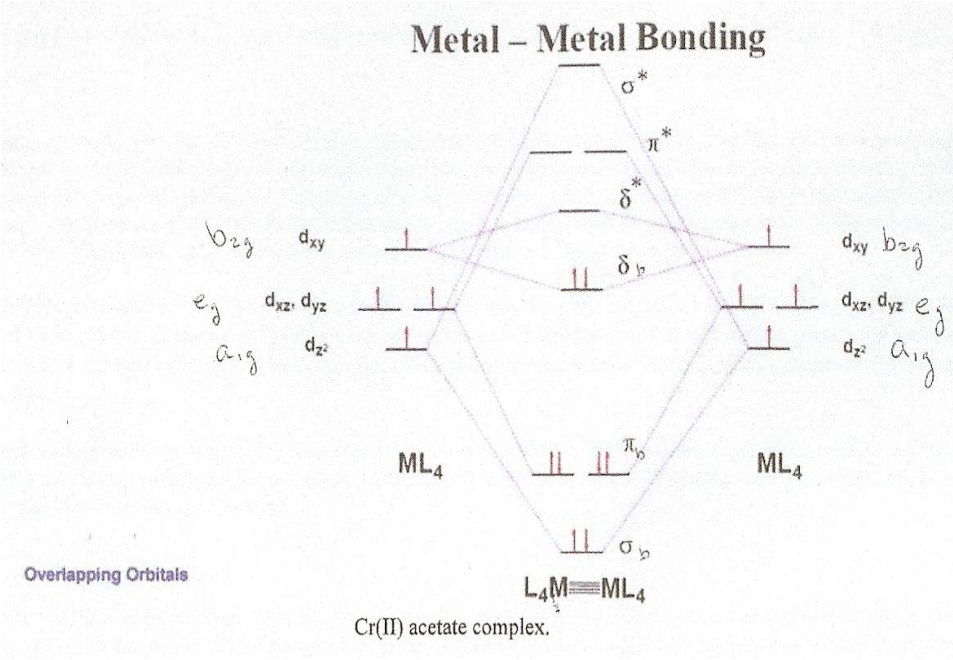

Figure 26. MO diagram for Cr (II) acetate complex[29]

Synthesis of $[Cr_2Mo(u_2\text{-}CH_3COO)_6(u_3\text{-}O)(H_2O)_3][CF_3SO_3]$

This preparation was very similar to that of $[Mo_3O_2(O_2CCH_3)_6(H_2O)(CF_3SO_2H)_2$ with the exception of using excess $Cr_2(OAc)_4$ in place of $Mo_2(O_2CCH_3)_4$. Finely ground $Na_2MoO_4{\cdot}2H_2O$ (1.20 g, 4.66 mmol) was placed in a solution of 70 ml acetic acid, 7 ml acetic anhydride and 1 ml triethyl amine utilizing the schlenk method. The suspension was deareated by purging with N_2 and brought to a reflux. The $Cr_2(OAc)_4$ dimer (2.0 g,

5.32 mmol) was added quickly under N_2 and refluxed for 11 days. After about 24 hours the solution changed to a dark brown color and all the solids had dissolved. After 4 days the solution changed to a medium purple color which indicated that product underwent oxidation. The synthesis was attempted again at increased temperature and longer reaction time. A green solution was achieved at higher temperature and 7 days of reflux. The solution was then vacuum filtered through a glass frit funnel and eluted through an acidified Dowex 50x2-200 cation exchange 15 cm height resin column. The eluent was slowly evaporated and produced a very small quantity of trigonal faced dark green octahedral crystals. The product was analyzed by utilizing three dimensional diffraction using Mo Kα radiation. The structure was confirmed to be crystals of the hetero-polynuclear metal complex $[Cr_2Mo(u_2\text{-}CH_3COO)_6(u_3\text{-}O)(H_2O)_3][CF_3SO_3]$. The complex was also analyzed using FTIR, CV and UV-VIS characterization methods.

III. RESULTS AND DISCUSSION

Electrochemistry of EMIBeti

EMIBeti is prepared by utilizing an ion exchange reaction with EMICl and LiBeti. EMICl is dissolved in 200 ml of H_2O after which an equal molar amount of lithium bis((pentafluoroethane)sufonyl)imide (LiBeti) dissolved in 200 ml of H_2O is added. After the reaction in solution has taken place the LiCl must be removed from the final product. The LiCl was completely removed by washing the solution with 40 ml of H_2O approximately 15 times. The solution was determined to be free of LiCl when it no longer tested positive when reacted with Ag^+. Once the solution was free of LiCl it was dried using high vacuum for removal of excess H_2O. IR spectra confirmed the identity of the ionic liquid. CV scans taken before and after washing the ionic confirmed all impurities had been removed. Figure 27 shows the inferred spectrum of EMIBeti after washing and drying the solution. The relatively small bands of H_2O stretching, at ~3600 cm^{-1} is observed. The two bands correspond to symmetric and antisymmetric stretching of H2O. If a larger amount of H_2O were present (> 300 ppm) a broad band at ~3400 cm^{-1} would be observed characteristic of the presence of hydrogen bonding.

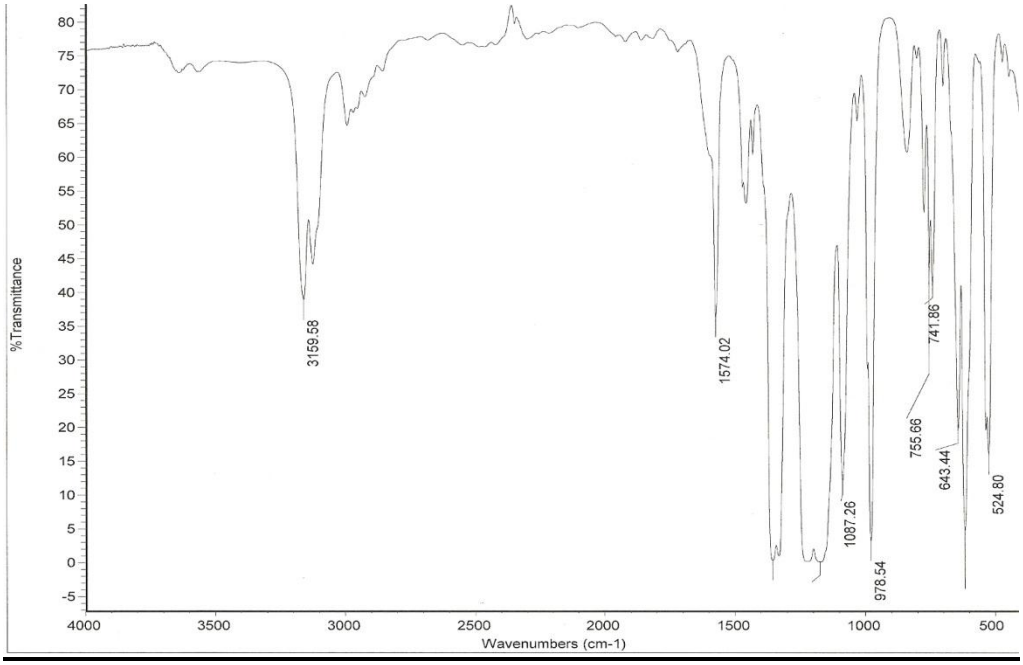

Figure 27. Infared spectrum of EMIBeti

CV scans taken of EMIBeti before and after purification confirmed the ionic liquid was clean and dry. Figure 28 shows the CV scan of the ionic prior to purifying. Figure 29 shows the CV scan of the ionic liquid post purification. The voltammogram does not show an oxidation peak at 1.0 V due to the oxidation of Cl^-. EMIBeti is known to have an electrochemical potential window of 4.3V with a positive potential of 2.1V and a negative potential of 2.2V.

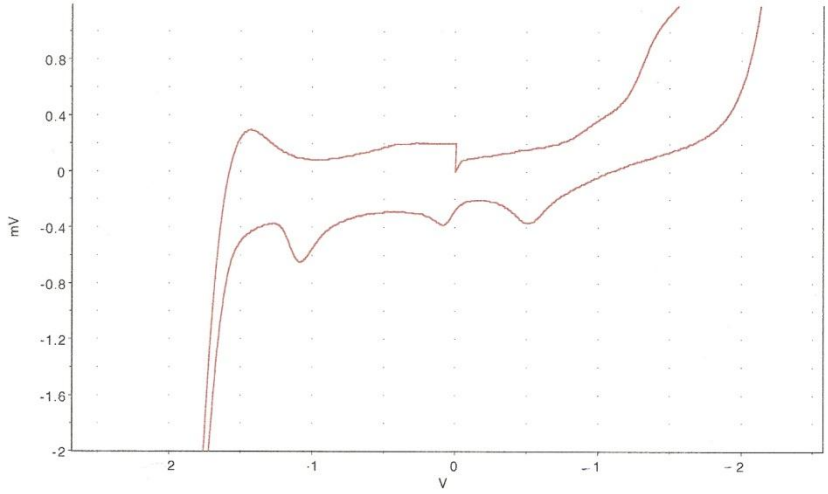

Figure 28. CV scan of EMIBeti with before purification

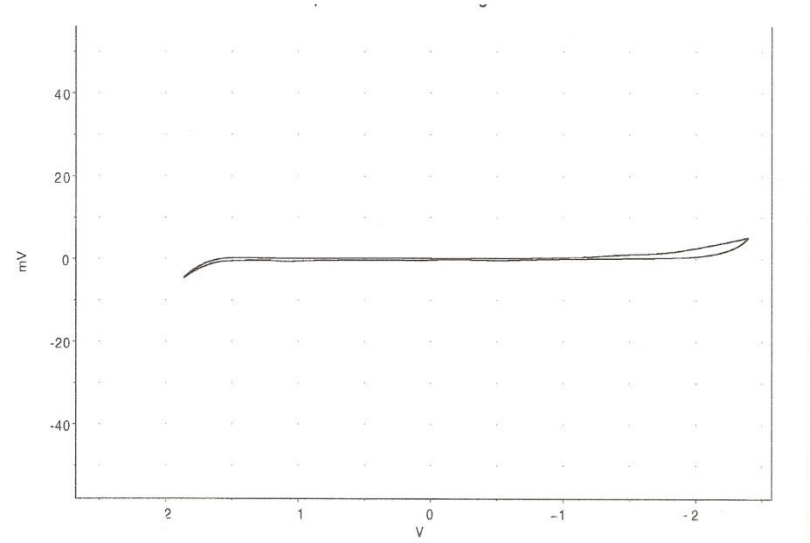

Figure 29. CV scan of EMIBeti after purification

For ionic liquids the electrochemical window is driven by the how much the cation can resist reduction and how well the anion can resist oxidation. Addition of a metal into the ionic liquid will reduce the electrochemical window of the ionic liquid. As an example ferrocene CV scans were ran in acetonitrile as shown in figure 30. Another CV scan of ferrocene was ran in EMIBeti as shown in figure 31 which clearly shows a reduction in the width of the electrochemical window.

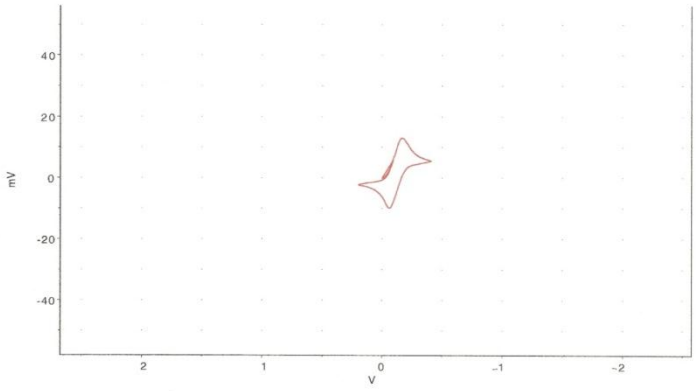

Figure 30. CV scan of Ferrocene in acetonitrile

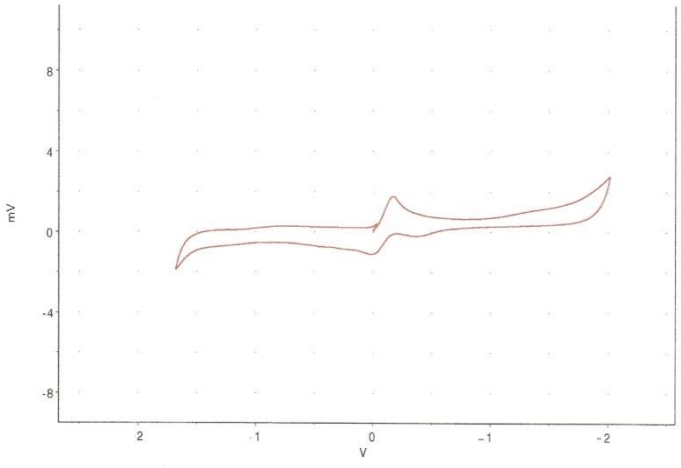

Figure 31. CV scan of Ferrocene in EMIBeti

Electrochemistry of trinuclear metal complexes

The electrochemical properties of $[Mo_3O_2(O_2CCH_3)_6(H_2O)(CF_3SO_2H)_2$ and $[Cr_2Mo(u_2\text{-}CH_3COO)_6(u_3\text{-}O)(H_2O)_3][CF_3SO_3]$ trinuclear metal complexes in ionic liquids were compared to their electrochemical properties in H_2O. The differences of structures of these two metal complexes are clearly shown in figure 32. The metal clusters, $[Mo_3O_2(O_2CCH_3)_6(H_2O)(CF_3SO_2H)_2$ and $[Cr_2Mo(u_2\text{-}CH_3COO)_6(u_3\text{-}O)(H_2O)_3][CF_3SO_3]$ do not readily dissolve in H_2O or EMIBeti. A small amount of each complex was placed in separate electrochemical cells equipped with tiny stir bars. Two samples of each metal complex were prepared, one containing H_2O and one containing EMIBeti. The samples were place on a stir plate at a temperature of 60^0 C for several days to dissolve the metal complexes. Electronic spectra of the metal complexes confirmed the structure of the metal complexes did not change by dissolving them in ionic liquid. Figure 33 shows the UV-Vis spectra of $[Mo_3O_2(O_2CCH_3)_6(H_2O)(CF_3SO_2H)_2$ dissolved in H_2O and figure 34 shows the UV-Vis spectra obtained in EMIBeti. Similarly, the electronic spectra of the $[Cr_2Mo(u_2\text{-}CH_3COO)_6(u_3\text{-}O)(H_2O)_3][CF_3SO_3]$ polynuclear complex obtained in H_2O and EMIBeti are shown in figure 35 and 36 respectively. The spectra are identical confirming that the metal complexes did not change by dissolving them in ionic liquid.

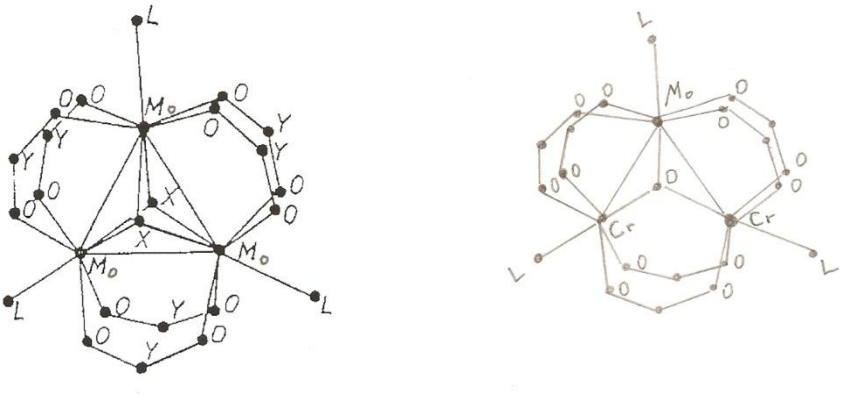

A. B.

Figure 32. A) $[Mo_3O_2(O_2CCH_3)_6(H_2O)(CF_3SO_2H)_2$ and B) $[Cr_2Mo(u_2\text{-}CH_3COO)_6(u_3\text{-}O)(H_2O)_3][CF_3SO_3]$.

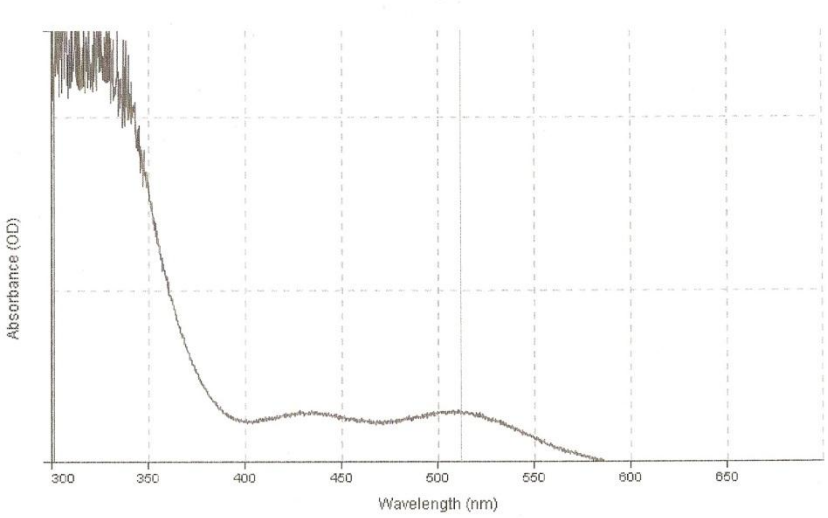

Figure 33. UV-Vis $[Mo_3O_2(O_2CCH_3)_6(H_2O)(CF_3SO_2H)_2$ in H_2O

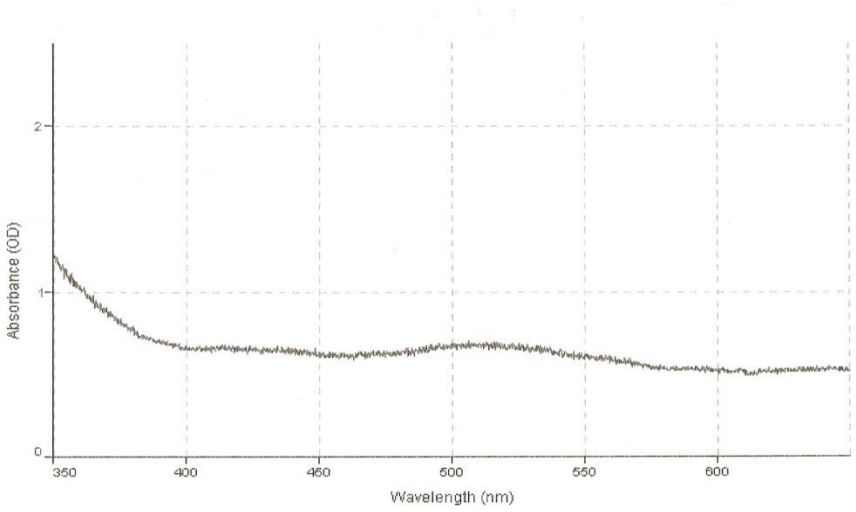

Figure 34. UV-Vis scan $[Mo_3O_2(O_2CCH_3)_6(H_2O)(CF_3SO_2H)_2$ in EMIBeti

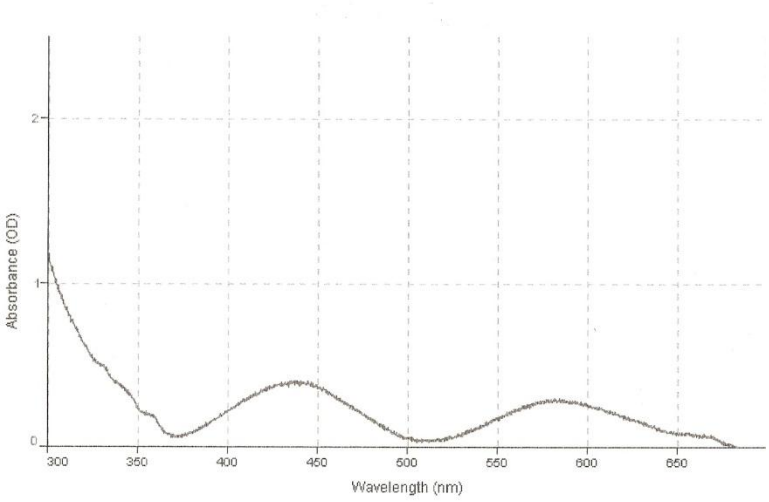

Figure 35. UV-Vis$[Cr_2Mo(u_2\text{-}CH_3COO)_6(u_3\text{-}O)(H_2O)_3][CF_3SO_3]$ in H_2O

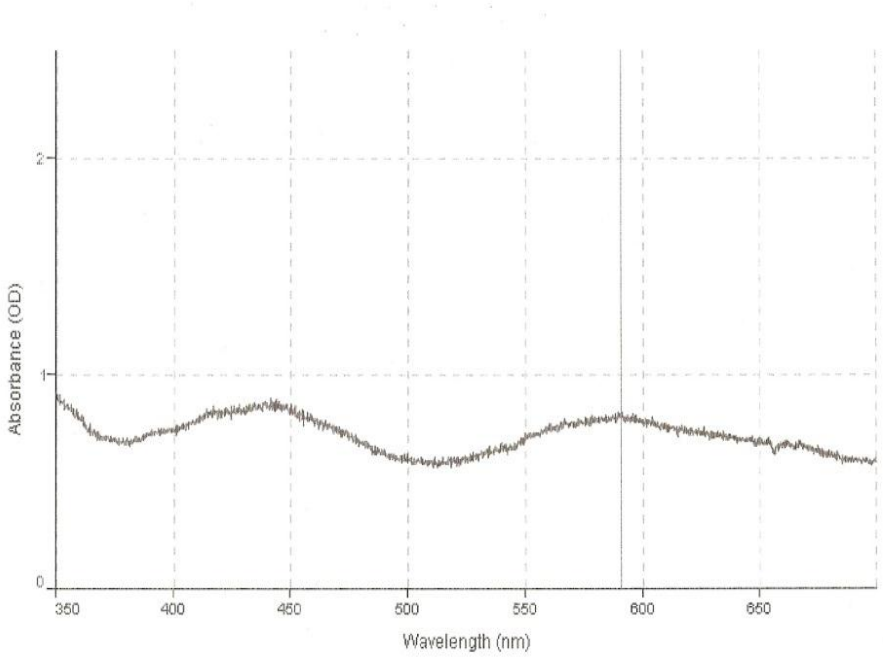

Figure 36. UV-Vis scan of $[Cr_2Mo(u_2\text{-}CH_3COO)_6(u_3\text{-}O)(H_2O)_3][CF_3SO_3]$ in EMIBeti

UV-Vis electronic spectra was obtained for the metal complex of $[Mo_3O_2(O_2CCH_3)_6(H_2O)(CF_3SO_2H)_2$ shows absorbance peaks at 435nm and 525nm in both H_2O and EMIBeti. The UV-Vis spectra for $[Cr_2Mo(u_2\text{-}CH_3COO)_6(u_3\text{-}O)(H_2O)_3][CF_3SO_3]$ metal complex gave absorbance peaks at 446nm and 535nm in both H_2O and EMIBeti.

Electrochemistry of $[Mo_3O_2(O_2CCH_3)_6(H_2O)(CF_3SO_2H)_2$

Cyclic volyammograms of $[Mo_3O_2(O_2CCH_3)_6(H_2O)(CF_3SO_2H)_2$ dissolved in EMIBeti ionic liquid using a platinum working electrode and a Ag/AgCl reference electrode are shown in figure 37. The voltammogram was initiated at 0 V, scanned in the negative direction and reversed at -1.9 V at a scan rate of 50 mV/sec. Figure 37 displays the reduction peak at -1.6 V and an oxidation peak at 1.1 V. A reverse CV in figure 38 displays an irreversible reduction peak at 1.23V with no oxidation peak during the cycle.

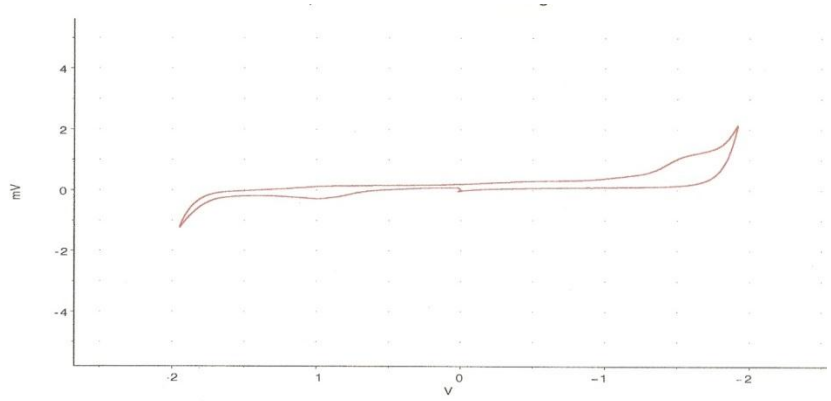

Figure37. Forward CV scan $[Mo_3O_2(O_2CCH_3)_6(H_2O)(CF_3SO_2H)_2$ in EMIBeti.

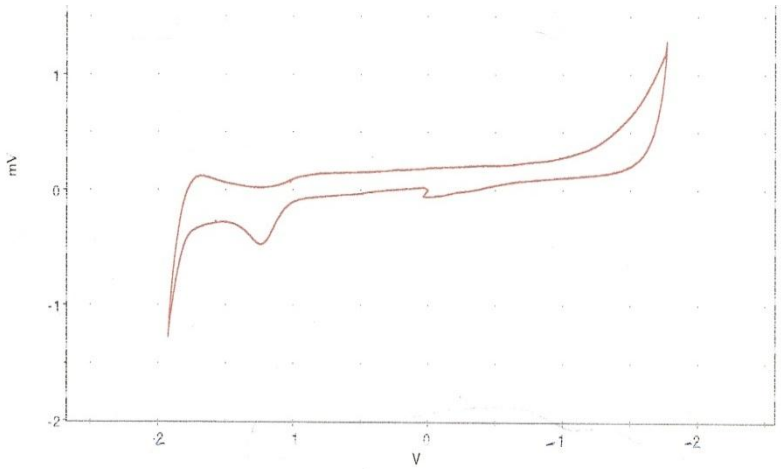

Figure38. Reverse CV scan of $[Mo_3O_2(O_2CCH_3)_6(H_2O)(CF_3SO_2H)_2$ in EMIBeti

Electrochemistry of $[Cr_2Mo(u_2\text{-}CH_3COO)_6(u_3\text{-}O)(H_2O)_3][CF_3SO_3]$

A structural study on $[Cr_2Mo(u_2\text{-}CH_3COO)_6(u_3\text{-}O)(H_2O)_3][CF_3SO_3]$ utilizing three dimensional diffraction using Mo Kα radiation has confirmed the configuration of the hetero-polynuclear cluster. The configuration of the complex cation consists of two chromium atoms and a single molybdenum atom in a triangular formation surrounding a single oxygen atom. The three metal atoms are each coordinated to the central oxygen atom, to four of the oxygen atoms of the acetate groups and to the oxygen of one of the water molecules. It appears as if the Mo is bonded to each of the chromium, but the chromium atoms are not directly bonded to each other in the octahedral formation. The acetate groups link the vertices of the central complex cation. The space group determined using Apex II software is the orthorhombic $P2_12_12_1$ due to the primitive orthorhombic nature of the crystal and the 2_1 screw axis along each x,y,z lattice directions. [1, 0, 0] at x, ¼, 0 with screw component [1/2, 0, 0], [0, 1, 0] at 0, y, ¼ with screw component ½-x, -y, ½ z, and [0, 0, 1] at ¼, 0, z with screw component [0, 0, ½]. Unit cell values resulted in a=12.72 Å , b=13.51 Å and c=16.92 Å where alpha, beta and gamma = 90^0. Z value calculated is 4, cell volume of 2909.1 with a density value of 1.729 g/$Å^3$ and a resolution factor value of 0.089. A comparison of the literature values [28] for trans-u_3-Oxo-tris{bisacetatoaquochromium(III) chloride hexahydrate is very similar where literature values were given as a=13.677 Å, b= 23.14 Å, c=9.14 Å with space groups as $P2_12_12_1$, V=2893.44, and Z=4. ρ was found to be 1.823 g/Å. Bond angles and distances were found to be in close range to literature [14] values reported as Cr to central O bond lengths of 1.95 Å, 1.86 Å and 2.04 Å compared to values determined here of Cr3-O2 = 1.89 Å, Cr8-O2 = 1.882 Å and Mo1-O2 = 1.909 Å. The following bond lengths for the hetero-central metal atoms were found to be, Mo1-Cr3=3.2877 Å, Mo1-Cr8=3.2815

Å. The angles between each metal atom found in the literature [28] were reported as Cr3-O4-Cr2=119.6 º, Cr2-O4-Cr1=118.9º and Cr1-O4-Cr3=121.6 º, compared to values reported here, found to be Cr3-O2-Mo1=119.3 º, Cr8-O2-Mo1=119.9 º, and Cr3-O2-Cr8=120.2 º. The solved structure is shown in figure 39.

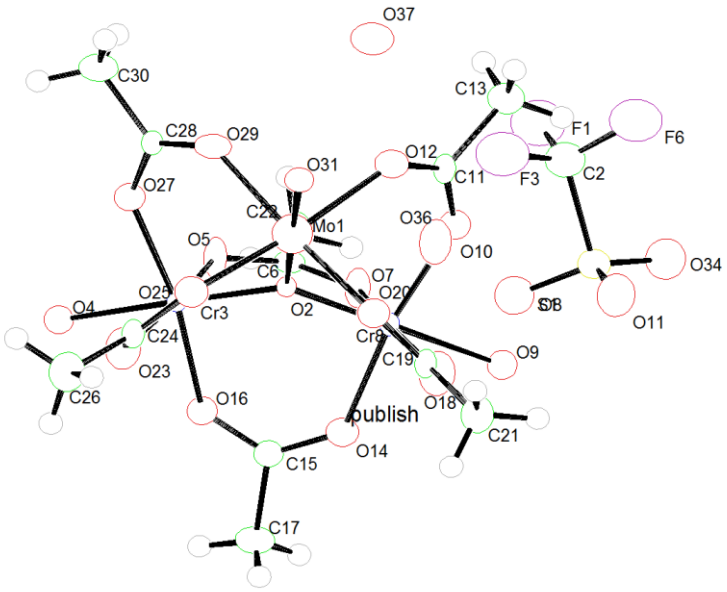

Figure 39. Structural solved for $[Cr_2Mo(u_2\text{-}CH_3COO)_6(u_3\text{-}O)(H_2O)_3][CF_3SO_3]$

Cyclic volyammograms of $[Cr_2Mo(u_2\text{-}CH_3COO)_6(u_3\text{-}O)(H_2O)_3][CF_3SO_3]$ dissolved in EMIBeti ionic liquid using a platinum electrode and a Ag/AgCl electrode are shown in figure 40. The voltammogram was initiated at 0, scanned in the negative direction and reversed at -1.9 V at a scan rate of 50 mV/sec and displays two reduction peaks at 0.85 V and 0.39 V. A single oxidation peak at -1.1 V appeared for the cycle. A reverse CV in figure 41 displays two irreversible reduction peaks at 1.05 V and 0.65 V, with no oxidation peak during the cycle.

The forward CV scan of $[Cr_2Mo(u_2\text{-}CH_3COO)_6(u_3\text{-}O)(H_2O)_3][CF_3SO_3]$ in EMIBeti is shown in figure 40. The reverse CV scan is shown in figure 41.

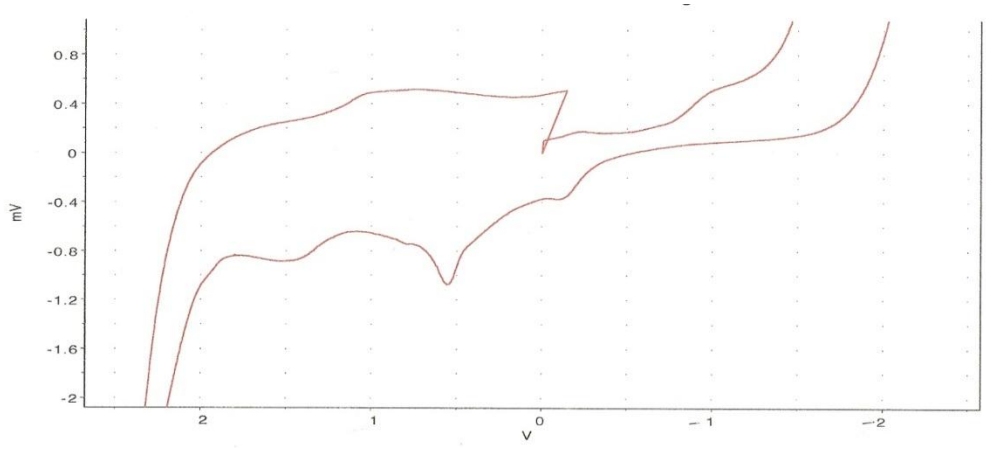

Figure 40. CV scan of $[Cr_2Mo(u_2\text{-}CH_3COO)_6(u_3\text{-}O)(H_2O)_3][CF_3SO_3]$ in EMIBeti.

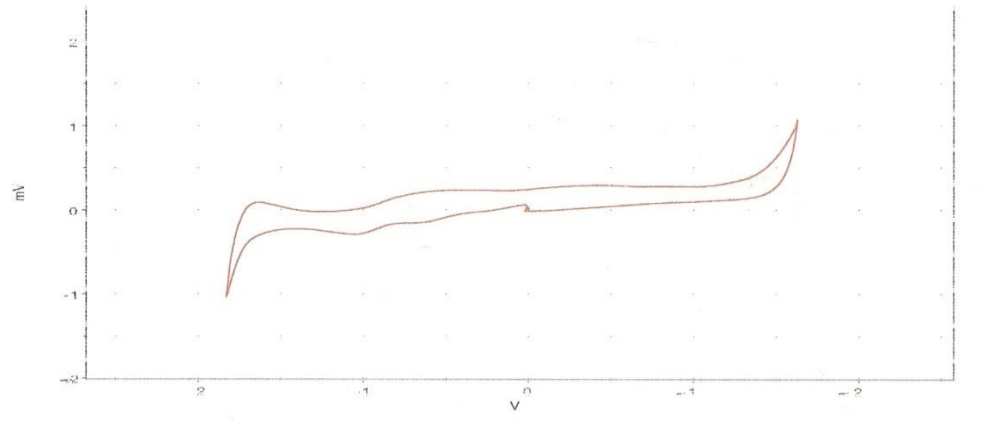

Figure 41. Reverse CV scan of $[Cr_2Mo(u_2\text{-}CH_3COO)_6(u_3\text{-}O)(H_2O)_3][CF_3SO_3]$ in EMIBeti.

IR spectra of $[Mo_3O_2(O_2CCH_3)_6(H_2O)(CF_3SO_2H)_2$ and $[Cr_2Mo(u_2\text{-}CH_3COO)_6(u_3\text{-}O)(H_2O)_3][CF_3SO_3]$ are shown in figures 42 and 43 respectively.

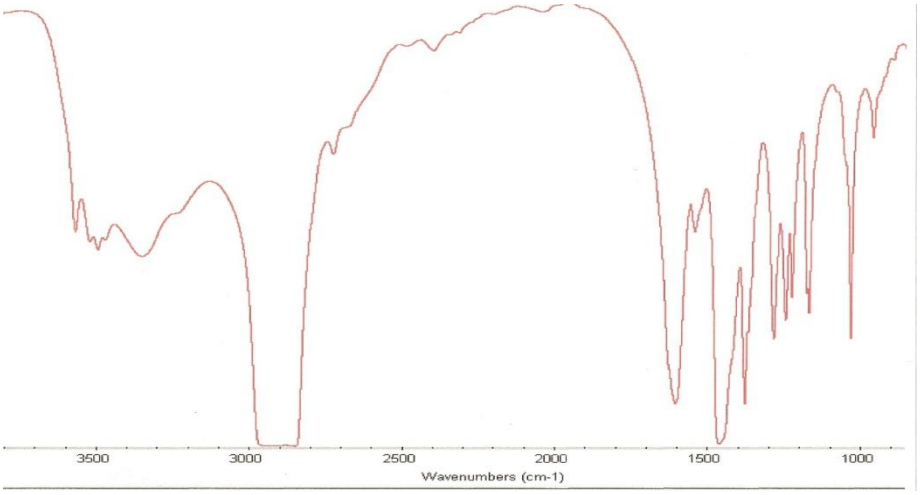

Figure 42. IR scan of $[Cr_2Mo(u_2\text{-}CH_3COO)_6(u_3\text{-}O)(H_2O)_3][CF_3SO_3]$

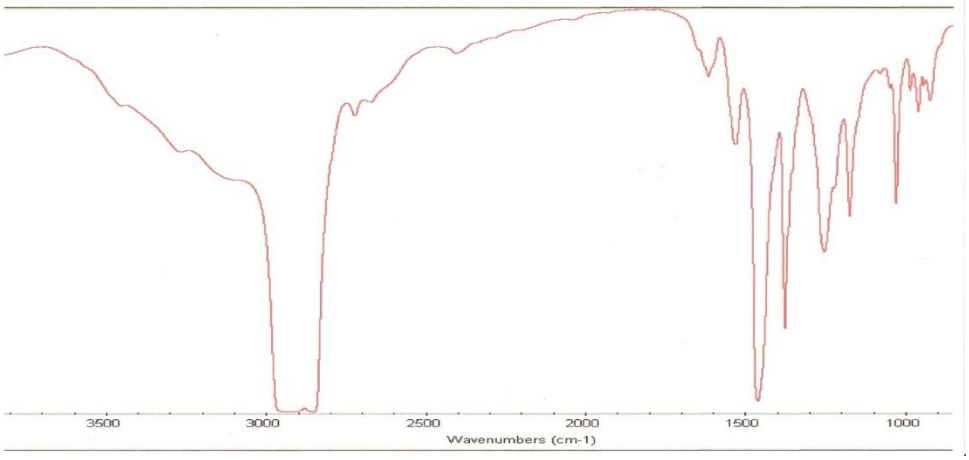

Figure 43. IR scan $[Mo_3O_2(O_2CCH_3)_6(H_2O)(CF_3SO_2H)_2$

Electrochemical deposition of $[Mo_3O_2(O_2CCH_3)_6(H_2O)(CF_3SO_2H)_2$ and $[Cr_2Mo(u_2\text{-}CH_3COO)_6(u_3\text{-}O)(H_2O)_3][CF3SO3]$ onto a Pt electrode

Based on the reduction potential indicated by the reverse sweep CV's, the two metal cluster complexes were chosen as comparison candidates for electrochemical deposition onto a pure Pt electrode. We propose that at a potential of-1.23 V, a complete reduction of the $[Mo_3O_2(O_2CCH_3)_6(H_2O)(CF_3SO_2H)_2$ cluster to metal using 12 electrons would take place.

$$[Mo_3O_2(O_2CCH_3)_6(H_2O)_3]^{2+} + 12e^- \rightarrow Mo_3$$

The deposition could be explained by the bonding of the metal atom of the Mo_3 cluster unit to the Pt. It has been proposed that the M_3 cluster in ionic liquid releases one H_2O molecule in the $[Mo_3O_2(O_2CCH_3)_6(H_2O)(CF_3SO_2H)_2$ cluster resulting in emptying one equatorial coordination site of the M_3 clusters available to bind to the Pt electron [24]. The result being easy transfer of electrons and formation of Mo deposition onto the Pt electrode. The proposed bonding is shown in figure 44.

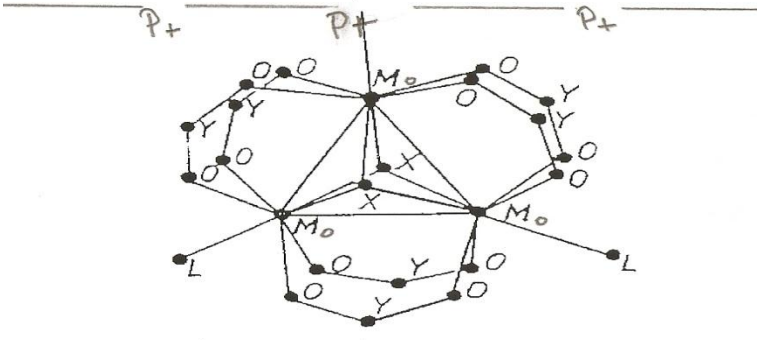

Figure 44. Proposed bonding between the M_3 cluster and platinum electrode.

The $[Mo_3O_2(O_2CCH_3)_6(H_2O)_3]$ metal species is made up of three direct metal-metal bonds and has a cation charge of +12. Each Mo atom has a formal oxidation state of +4. However, in the metal complex of $[Cr_2Mo(u_2\text{-}CH_3COO)_6(u_3\text{-}O)(H_2O)_3]$ species the Mo is directly bonded to each of the Cr atoms but the Cr atoms do not bond to each other. There is also a difference in the charge of the cation for of $[Cr_2Mo(u_2\text{-}CH_3COO)_6(u_3\text{-}O)(H_2O)_3]$ where the Mo has an oxidation state of +4 but each of the Cr atoms only carry a charge of +3 which gives an formal oxidation state of 3.33 for the metal center. The bond distances found for the Mo_3 species are also different. Mo_3 complexes are reported as 2.46 Å to 2.55 Å[17]. According to the crystallography data obtained for $[Cr_2Mo(u_2\text{-}CH_3COO)_6(u_3\text{-}O)(H_2O)_3]$ the bond distance between the Mo atom and each of the two Cr atoms was found to be approximately 3.3 Å which would result in a much weaker bond [23]. To investigate the deposition of each metal complex onto a Pt electrode, a constant reduction potential on a small Pt foil electrode was performed. A two compartment electrochemical cell was used for the electrodeposition of each species. A pure Pt foil working electrode and an Ag/AgCl reference electrode were placed in the cathodic compartment. The auxiliary Pt electrode was placed in the anodic compartment. A solution of $[Mo_3O_2(O_2CCH_3)_6(H_2O)_3]$ metal species dissolved in EMIBeti was electrolyzed at -1.23 V for 50 hours. Inspection of the Pt electrode using scanning electron microscopy (SEM) indicates that a deposition had occurred. Furthermore, energy dispersion spectroscopy (EDS) indicated a definite change in the metal composition of the pure Pt foil electrode. The initial composition of the Pt foil electrode was 100% compared to 88.1% for Pt post deposition and 1.59% for the amount of Mo on the same electrode. Figure 45 shows the SEM images of the Pt electrode before and after the electrochemical deposition of

$[Mo_3O_2(O_2CCH_3)_6(H_2O)_3]$ onto the Pt electrode. Figure 46 shows the results of the EDS analysis performed on the same Pt electrode post electrochemical deposition.

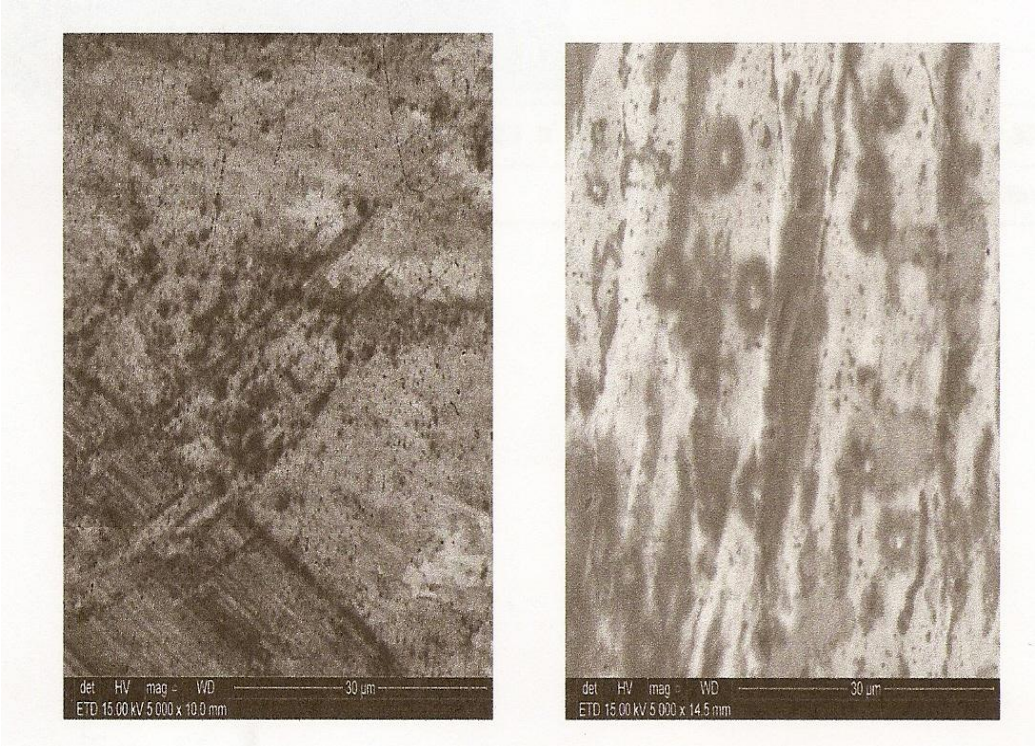

A. Pre-electrochemical deposition B. Post- electrochemical deposition

Figure 45. SEM 5000x of Pt electrode A.) Pre-electrochemical deposition , B.) Post-electrochemical deposition of $[Mo_3O_2(O_2CCH_3)_6(H_2O)(CF_3SO_2H)_2$

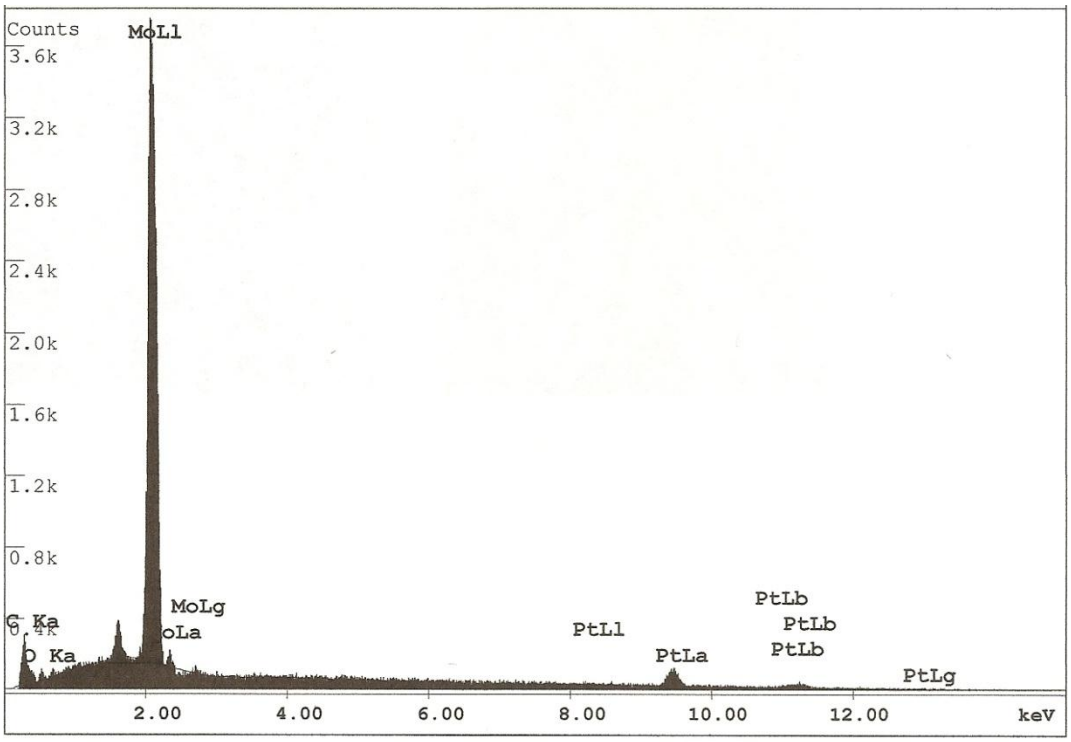

EDAX ZAF Quantification (Standardless)
Element Normalized
SEC Table : Default

Element	Wt %	At %	K-Ratio	Z	A	F
C K	9.13	58.18	0.0213	1.3856	0.1683	1.0000
O K	1.26	6.04	0.0028	1.3565	0.1632	1.0000
MoL	1.59	1.27	0.0079	1.0541	0.4722	1.0000
PtL	88.01	34.51	0.8020	0.9076	1.0040	1.0000
Total	100.00	100.00				

Element	Net Inte.	Bkgd Inte.	Inte. Error	P/B
C K	13.75	1.45	2.97	9.48
O K	3.46	3.75	9.57	0.92
MoL	4.07	14.08	13.95	0.29
PtL	13.69	3.26	3.28	4.20

Figure 46. Data from Energy Dispersion x-ray diffraction scans for Pt electrode post $[Mo_3O_2(O_2CCH_3)_6(H_2O)(CF_3SO_2H)_2$ electrochemical deposition.

CV scans of the remaining solution in the electrochemical cell was performed and it is clearly show in figure 47 that the forward scan no longer gives evidence of presence of the $[Mo_3O_2(O_2CCH_3)_6(H_2O)$ species. UV-Vis scans were also taken of the solution post electrochemical deposition and are shown in figure 48. A band shift toward a lower frequency and longer wavelength indicates a change in the composition of the species in the solution.

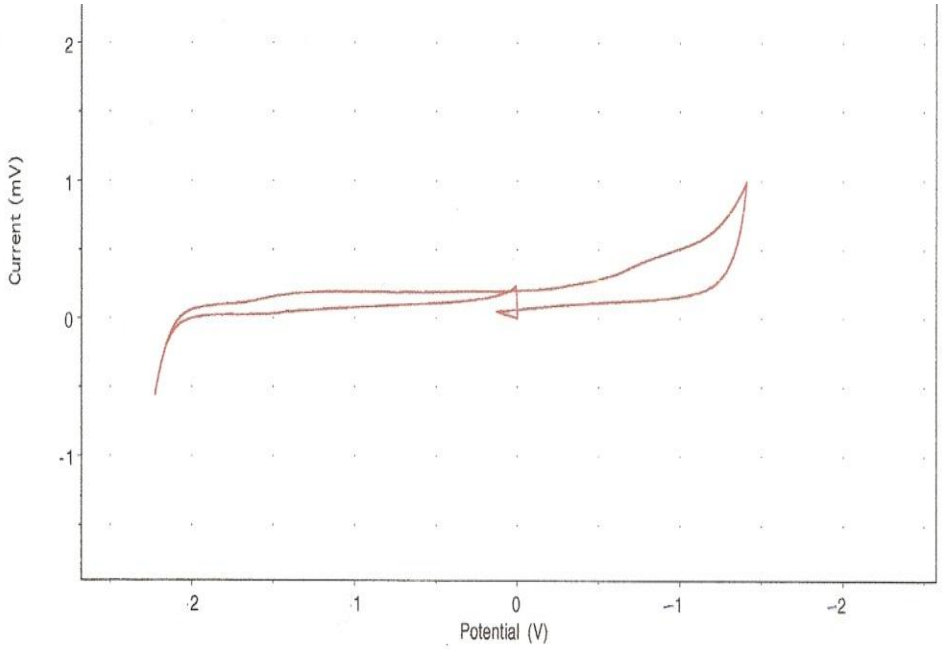

Figure 47. CV scan post electrochemical deposition of $[Mo_3O_2(O_2CCH_3)_6(H_2O)$ in EMIBeti.

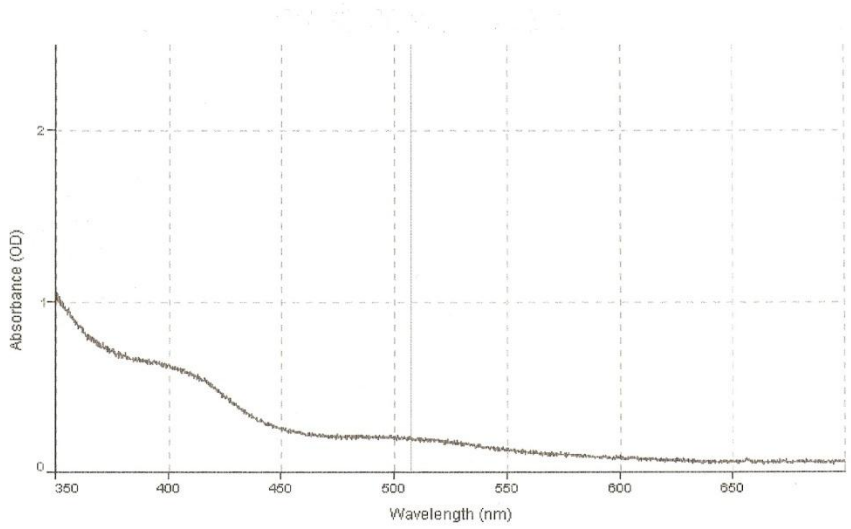

Figure 48. UV-Vis scan of $[Mo_3O_2(O_2CCH_3)_6(H_2O)(CF_3SO_2H)_2$ post electrochemical deposition.

Similarly, using the same type of electrochemical cell, an attempt was made to electrochemically deposit $[Cr_2Mo(u_2\text{-}CH_3COO)_6(u_3\text{-}O)(H_2O)_3$ in EMIBeti onto the Pt electrode. The only difference being the value of the applied potential, -1.05 V at which the $[Cr_2Mo(u_2\text{-}CH_3COO)_6(u_3\text{-}O)(H_2O)_3$ species was electrolyzed. The Inspection of the Pt electrode using scanning electron microscopy (SEM) indicates that no deposition of $[Cr_2Mo(u_2\text{-}CH_3COO)_6(u_3\text{-}O)(H_2O)_3$ had occurred. Furthermore, energy dispersion spectroscopy (EDS) indicated a change in the metal composition of the pure Pt foil electrode had not occurred. The initial composition of the Pt foil electrode was 100% and remained the same for the Pt electrode post attempted electrodeposition. Figure 49 shows the SEM images of the Pt electrode before and after the electrochemical deposition of $[Cr_2Mo(u_2\text{-}CH_3COO)_6(u_3\text{-}O)(H_2O)_3$. There is a difference of appearance for the Pt electrode, however the EDS in figure 50 shows no signs of the presence of either Cr or

Mo atoms. CV scans of the remaining solution in the electrochemical cell was also performed and clearly show in figure 51 that the forward scan gives evidence that the $[Cr_2Mo(u_2\text{-}CH_3COO)_6(u_3\text{-}O)(H_2O)_3$ species is still present in the electrolyzed solution. UV-Vis scans were also taken of the solution post electrochemical deposition and are shown in figure 52. Characteristic peaks for $[Cr_2Mo(u_2\text{-}CH_3COO)_6(u_3\text{-}O)(H_2O)_3$ were not present which possibly indicate that the species basically fell apart while undergoing electrolyzation.

A. Pre-electrochemical deposition B. Post- electrochemical deposition

Figure 49. SEM scan 5000x of Pt electrode A.) Pre-electrochemical deposition

B.) Post- electrochemical deposition of$[Cr_2Mo(u_2\text{-}CH_3COO)_6(u_3\text{-}O)(H_2O)_3][CF_3SO_3]$

$Cr_2Mo(u_2\text{-}CH_3COO)_6(u_3\text{-}O)(H_2O)_3$

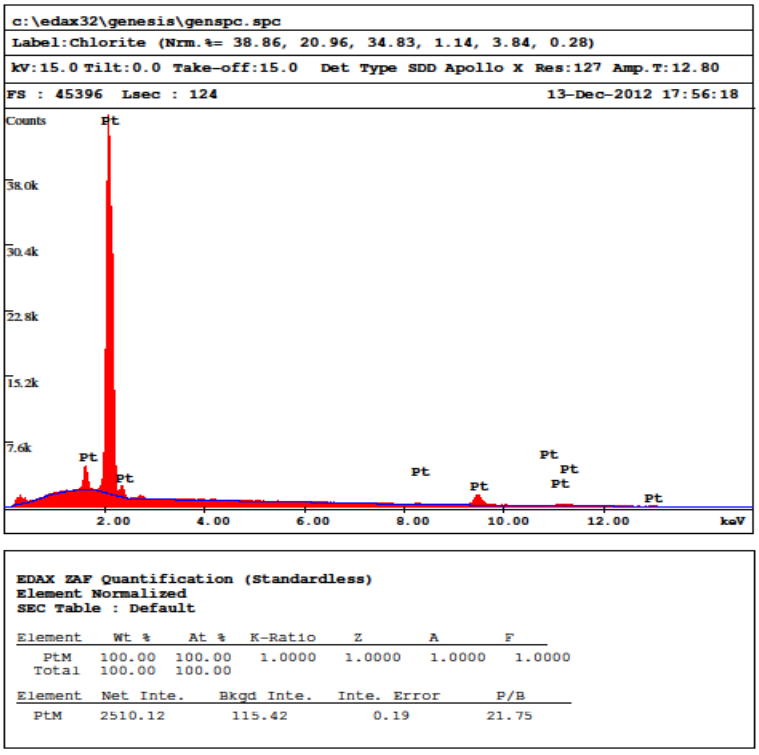

Figure 50. Data from Energy Dispersion x-ray diffraction scans for PT electrode post $[Cr_2Mo(u_2\text{-}CH_3COO)_6(u_3\text{-}O)(H_2O)_3][CF_3SO_3]$ electrochemical deposition attempt.

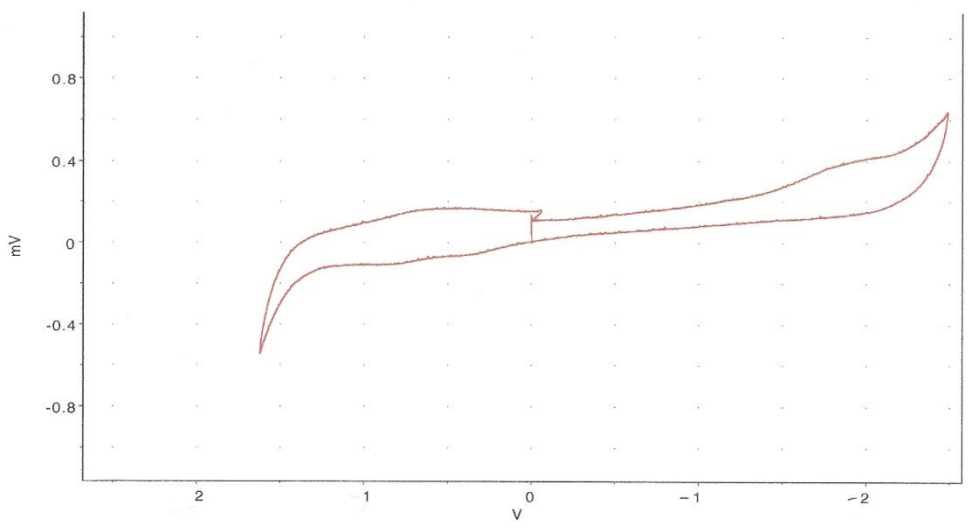

Figure 51. CV scan of of $[Cr_2Mo(u_2\text{-}CH_3COO)_6(u_3\text{-}O)(H_2O)_3][CF_3SO_3]$ post electrochemical deposition.

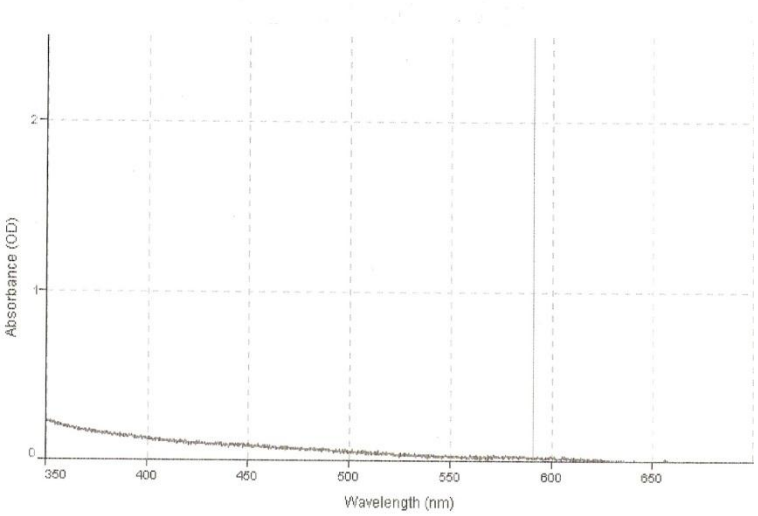

Figure 52. UV-Vis scan of of $[Cr_2Mo(u_2\text{-}CH_3COO)_6(u_3\text{-}O)(H_2O)_3][CF_3SO_3]$ post electrochemical deposition.

IV. CONCLUSION

In this work the electrochemical properties of two different types of metal clusters was investigated in an attempt to modify a Pt electrode. The trinuclear homogeneous metal cluster of $[Mo_3O_2(O_2CCH_3)_6(H_2O)(CF_3SO_2H)_2$ and the polynuclear metal complex $[Cr_2Mo(u_2\text{-}CH_3COO)_6(u_3\text{-}O)(H_2O)_3][CF_3SO_3]$ in EMIBeti ionic liquid were both thought to be good candidates due to thier early transition metal and electrochemical potential characteristics. EMIBeti was chosen as a suitable electrolyte solution due to its stability and wide electrochemical potential window. Modification of a Pt electrode using metal cluster compounds is thought to enhance the catalytic properties of the Pt electrode.

It was shown by UV-Vis that the species of both the metal complexes maintain their chemical integrity when dissolved in EMIBeti. After electrochemical deposition experiments of both metal complexes it was found that the trinuclear metal cluster of $[Mo_3O_2(O_2CCH_3)_6(H_2O)(CF_3SO_2H)_2$ could be successfully deposited onto a Pt electrode but the polynuclear complex of $[Cr_2Mo(u_2\text{-}CH_3COO)_6(u_3\text{-}O)(H_2O)_3][CF_3SO_3]$ could not be deposited. The successful deposition was proven by SEM and EDS spectroscopy methods.

Research could be extended further by actually using the modified Pt electrode in a fuel cell such as an ethanol fuel cell to enhance the fuel cells ability to make the reaction that takes place procede to completion. This

would be a benefit for the utilization of ethanol as an alternative energy resource.

I. REFERENCES

1. Wilkies, J.S.; Zaaworotko, M.J. *J. Chem.Soc.Chem.Commum.* **1992**, 965.
2. Hussey, C.L. and Marassi, R. *Techniques for characterization of electrodes and electrochemical processes*. John Wiley& Sons, Inc., New York, **1991**
3. Freemantle, M. *Chem. Eng. News*, (March 30) **1998**, 76, 32.
4. Dancevic, A. *Synthesis and Purification of Imidazolium and Pyrazolium based Ionic liquids and their Applications in Electrochemistry*. WSU, **2003**
5. Earle, M. J; Seddon, K.R. *Pure Appl. Chem*. **2000**, 1391.
6. Wasserscherd, P.; Welton, T. *Ionic liquid synthesis*. Wiley –Vch, Verlag, **2003**
7. Chen, Po-Yu; Sun,I-Wen,"Electrochemistry of Cd(II) in the basic 1-ethyl-3-methylimidazolium chloride/tetrafluoroborae Room Temperature Molten Salt" *Electrochimica Acta* **2000**, 3163-3170
8. F. A. Cotton, ***Accounts Chem. Res.,*** 2,240 (**1969**).
9. Huheey, J.E;. Keiter, E.A.; Keiter; R.L. "*Inorgnic Chemistry*" forth edition **1993**
10. L. Pauling, " *The Nature of the Chemical Bond*" , 3rd. , Cornell University Press, Ithaca N.Y., **1960**
11. Geilnann, W.; Wriuce, F. W.; Biltz. W.: *Nachr. Ges. Wiss. Gottingen* **1932**, 579.

12. Syzuki,T.,*TriNuclear Mixed Metal Clusters of Molybdenum and Tungsten,*WSU **1985**

13. *Annu. Rep. Prog. Chem.*, Sect. A, **2002**, 98, 153-17

14. Keith J. Laidler and J.H. Meiser, *Physical Chemistry*, Benjamin/Cummings (**1982**), p.423

15. M. G.Thhomas, B. F. Beier, E. L. Muetteries, *J. Am. Chem. Soc*., 98, 24, 241, (**1985**).

16. A. Bino, F.A. Cotton, Z. Dori, S. Koch, H. Kruppers, M. Miller, *Inorg. Chem*., 17, 3245, (**1978**).

17. . F. A. Cotton, Z. Dori, D. O. Marler, W. Schwotzer, *Inorg. Chem*., **1983**, 22, 3104-3106.

18. Williams, M. H., *Electrochemical Investigation of Transition Metal Complexes in Imidazolium based Ionic Liquids,* WSU, **2006**

19. R. E. M^{c}Carley, J. L. Templeton, T. J. Colburn, V. Katovic, R. J. Hoxeier, *Adv. Chem. Ser.* No. 150, 318, (**1976**)

20. Jolly,William L., "*The Synthesis and Characterization of inorganic Compounds*", Princeton-Hall, Inc. – Library of Congress II, 78-100587, 442-44

REFERENCES CONTINUED

21. Harris, T. *Electrochemistry of Trinuclear Metal Clusters of Molybdenum and Tungsten in 1-Ethyl-3-Methylimidazolium Tetrafluoroborate*. WSU, **2008**.

22. D. M. P. Mingos, David J Wales , *Introduction to cluster chemistry*, Prentice-Hall, **1990**, ISBN 0-413-499049-9

23. Woods ,C. J., *Electrochemical Deposition Of Molybdenum And Tungsten From Trinuclear Metal Clusters* $Mo_3O_2(OAc)_6(H_2O)_3(CF_3SO_3)_2$ *In 1-Ethyl-3-Methylimidazolium Tetrafluoroborate Ionic Liquid.* WSU, **2010.**

24. Scanning Electron Microscopy images and profile measurements provided by WPAFB.

25. Conner, J. A. *Top. Curr. Chem.* **1977,** *71*, 71.

26. Kubas, G. J. and van der Sluys, L. S., "TriscarbonlylTris(nitrile) Complexes of Cr, Mo, and W", *Inorganic Synthesis*, **1990**, 28, 29-33, ch6.

27. Girolami, S. G., Rauchfuss T. B., Angelica,R. J., *"Synthesis and Technique in inorganic Chemistry*": A laboratory manual- 3rd ed., University Science Books, **1999**, *11*, 111.

28. Chang, S. C., Jeffery, G. A., "The Crystal Structure of a Basic Chromium Acetate Compound, $[OCr_3(CH_3COO)_6.3H_2O]^+Cl^-.6H_2O$, havinf feeble Paramagnetism" *Acta Cryst.* **1970**, B26, 673.

29. F. A., Cotton, Murillo C. A., Walton R. A., "*Multiple Bonds between Metal Atoms*" Springer Science and Business Media Inc., New York **2005**, 31,3.13.

30. Bruker (2007). *APEX2*. Bruker AXS Inc., Madison, Wisconsin, USA.

31. Patrick McArdle, Karen Gilligan, Desmond Cunningham, Rex Dark and Mary Mahon *CrystEngComm*, 2004, 6, 303 – 309

32. Kissinger, P. T., Heineman, W. R., "*Laboratory Techniwues in Electroanalytical Chemistry"* Marcel Dekkar Inc. New York, New York **1984,** 82-100.